Code Division Multiplexing of Fiber Optic and Microelectromechanical Systems (MEMS) Sensors

Carl P. Jacobson

Dissertation submitted to the Faculty of the
Virginia Polytechnic Institute & State University
in partial fulfillment of the requirements for the degree of

Doctor of Philosophy
in
Electrical Engineering

Richard O. Claus, Chair
Guy J. Indebetouw
G.Q. Lu
Wing F. Ng
Kent A. Murphy

May 2, 2000
Blacksburg, Virginia

Keywords: Fiber Optics, MEMS, Sensor, Multiplexing

Code Division Multiplexing of Fiber Optic and Microelectromechanical Systems (MEMS) Sensors

Carl P. Jacobson

(ABSTRACT)

Multiplexing has evolved over the years from Emile Baudot's method of transmitting six simultaneous telegraph signals over one wire to the high-speed mixed-signal communications systems that are now commonplace. The evolution started with multiplexing identical information sources, such as plain old telephone service (POTS) devices. Recently, however, methods to combine signals from different information sources, such as telephone and video signals for example, have required new approaches to the development of software and hardware, and fundamental changes in the way we envision the basic block diagrams of communication systems. The importance of multiplexing cannot be overstated. To say that much of the current economic and technological progress worldwide is due in part to mixed-signal communications systems would not be incorrect.

Along the vein of advancing the state-of-the-art, this dissertation research addresses a new area of multiplexing by taking a novel approach to network different-type sensors using software and signal processing. Two different sensor types were selected, fiber optics and MEMS, and were networked using code division multiplexing. The experimentation showed that the interconnection of these sensors using code division multiplexing was feasible and that the mixed signal demultiplexing software unique to this research allowed the disparate signals to be discerned. An analysis of an expanded system was performed with the results showing that the ultimate number of sensors that could be multiplexed with this technique ranges from the hundreds into the millions, depending on the specific design parameters used. Predictions about next-next generation systems using the techniques developed in the research are presented.

Acknowledgments

I would like to thank my advisor: Richard O.Claus and committee members Kent. A. Murphy, G.J. Indebetouw, G.Q. Lu, and W.F. Ng. Their encouragement along the way has made it possible for me to complete this dissertation.

I would like to thank my father for his support and assistance and also my sister, her husband and their three children for their encouragement, too.

I would like to thank the many managers and supervisors who have encouraged me in this effort, and, perhaps more importantly, signed off on those tuition payment forms.

This dissertation is dedicated to the memory of my mother, Anna Marie Jacobson who encouraged me in this effort.

Table of Contents

List of Figures

List of Tables

Chapter 1 - Introduction

Multiplexing is defined as simultaneously communicating two or more messages on the same channel. One has only to look at the communications technology that surrounds us to realize that multiplexing is everywhere. The car radio carries several different signals at once as does the television and the Internet. Combining signals onto one media has resulted in a new society, one where the participants can communicate effectively and easily.

The first person to implement multiplexing was Emile Baudot in 1874 [1.1]. His system enabled telegraphers to send 6 signals simultaneously over one line. Later, Marconi developed a means for sending signals over the airwaves by using a spark gap transmitter operating on a specific frequency. This paved the way for other transmitters and receivers to be used simultaneously, each operating on its own frequency. In effect, the modern broadcast world uses multiplexing to allow many stations to broadcast over the same media, the airwaves. Multiplexing is a key ingredient in internetworking, which is described as collection of individual networks, connected by intermediate networking devices, that functions as a single large network [1.2].

Three common forms of multiplexing are Frequency Division Multiplexing (FDM), sometimes called Wavelength Division Multiplexing (WDM), Time Division Multiplexing (TDM) and Code Division Multiplexing (CDM). With FDM, different signals are separated by frequency. AM broadcasting is an example of FDM, where one hears a station at 810 kHz, another at 820 kHz another at 830 kHz and so on. With TDM the signals are transmitted at different times rather than different frequencies (Baudot's code mentioned above was a form of TDM), and with CDM, each signal possesses a different code and the detector (receiver) is trained to look for that particular code.

Each form of multiplexing has its own advantages and disadvantages and lends itself to a particular application. FDM is used for analog cellular communications as well as for optical fiber communications. TDM is used for digitial cellular communications and for both optical

fiber and electronic communications of a digital nature. CDM is used for Personal Communications Systems (PCS) and is perhaps the fastest growing form of multiplexing. Originally devised during World War II for use in RADAR, it saw limited use until the development of PCS. It provides for a good signal to noise ratio and increased security [1.3].

As computing power has increased over the years, so has the use of computers and software to achieve multiplexing goals. For example today, the CISCO router uses both hardware and software to achieve the multiplexing required for the Internet. Additionally, CDM makes use of the increased processing power to form its long codes and algorithms.

The aforementioned examples of multiplexing use identical information sources; that is voice is multiplexed with voice, digital data with digital data and so forth. However, the current challenge to connecting various systems is to support communication between disparate technologies [1.2] and recently effort has been made to multiplex different signals together. This is the primary concept involved with the highly successful CISCO Company and their mixed signal routers. Multiplexing different types of signals is one reason the Internet has expanded and continues to bring new possibilities of communications to the consumer. In fact, the high speed multiple access communication systems now form the basis of much of the current economic and technical progress worldwide.

Taking this concept one step further is combining signals from different sources, such as different types of sensors. To do this on a large scale would allow a further expansion of communications. However, this is one area of multiplexing where little if anything has been done. The idea of combining signals from totally different devices has not been explored. This area of research is just as fundamental as multiplexing communications signals, but may be more difficult to envision because the number of possible sensor devices is large. In this dissertation research, I have chosen two physical devices, optical fiber sensors, and electronic sensors (MEMS) as inputs and I have used software in the form of code division multiplexing and hardware design to multiplex these sensors.

The technical barriers analyzed in this dissertation research are similar to multiplexed communications systems. The primary limit is the number of sensors one can multiplex on a network. That limit affects a number of interrelated parameters such as network topology, physical device limitations, code size, code configuration, increased complexity of the sensor devices, bit error rate limitations on sensor resolution and response time of the sensor network.

The dissertation is organized as follows: Chapter 2 discusses code division multiplexing as applied to fiber optic sensors. Chapter 3 discusses MEMS technology in a general sense, giving examples of MEMS products and the procedures used in MEMS manufacturing. A systems analysis and design is presented in Chapter 4. The integration of the MEMS and fiber optic sensors along with the experimental results are discussed in detail in Chapter 5. Chapter 6 is an analysis and discussion of system limitations. An example of Naval Shipboard Multiplexed Sensor Networks is presented in Chapter 7 and conclusions are in Chapter 8.

Chapter 2 - Code Division Multiplexing

The heart of this research lies in the multiplexing algorithms. In order to network different-type sensors it is necessary to explore successful multiplexing methods that have been used on same-signal devices. Code division multiplexing has been used to multiplex same-signal communications devices for some time. Closely related research has resulted in the multiplexing of fiber optic sensors onto the same network. Given the enormity of the work that has recently transpired in fiber optic sensors [2.1-2.16], this makes sense. In this chapter, this same-signal multiplexing work is explored with the idea of expanding it to a more desirable mixed-signal network.

2.1 Code Division Multiplexing History

Code division multiplexing utilizes pulse compression and cross-correlation techniques, originally developed for radar, to reduce signal to noise ratios [2.17]. The technology provides for the increase of the number of optical sensors one can monitor with a single optical source. It was adapted to multiplexing optical sensors on an experimental basis starting in the 1980's [2.18-2.22]. It is also used in cellular telephone networks where it is called Code Division Multiple Access (CDMA)

2.2 Pseudorandom Bit Sequences

At the heart of code division multiplexing is the pseudorandom bit sequence which is a series of pulses that appear to mimic white noise. These lend themselves to being incorporated into digital signal processing. A maximal length pseudorandom bit sequence is one that has a length of $2^m - 1$ where m is an integer. Maximal length pseudorandom bit sequences satisfy certain postulates of randomness. They are:

1. In every sequence period, the number of +1's shall not differ from the number of -1's by more than one.
2. For every sequence period, half of the runs (a run being a subsequence of -1 or +1) have a length of one, 1/4 of the runs have a length of 2, 1/8 of the runs have a length of 3 and so on as long as the number of runs exceeds one. Furthermore, for each of the runs there are equally many runs of +1's and -1's.
3. The autocorrelation function is binary valued; that is

$$R(m)=p,\ m=0, \tag{2.1.1}$$

$$R(m)=c,\ 0<|m|<p. \tag{2.1.2}$$

We desire $p \gg c$ so the sequences look white [2.23]. The autocorrelation function for a 7 bit length code is shown in Figure 2-1.

2.3 Code Generation

Code generation is key to this form of multiplexing. These are typically generated in hardware, by the use of clocks and logical flip-flop circuits. Figure 2- 2(a) [2.17] shows the design of a code generator made up of a 3 stage shift register. The pseudorandom pulse sequence repeats every 7 pulse times, labeled T in Figure 2-2(b) [2.17]. The pulses are also polar binary, meaning they return to a negative number, not to zero. The calculated autocorrelation functions, shown below, for both a single optical sensor and for 3 optical sensors repeats every 7 pulse times. Three sensors are the maximum number of sensors that can be interrogated for a 3 stage shift register, because each correlation function requires 2 pulse times and the sequence repeats every 7 pulse times.

Calculating the autocorrelation function is simply a matter of adding the number of agreements and then subtracting the number of disagreements as the code is compared with itself. For

example, with a 3 stage register, the code that is generated is 0111001. If one compares this code with an identical code, the number of agreements is 7, i.e. 0 agrees with 0, 1 agrees with 1, 1 agrees with 1, and so on. The number of disagreements is 0. If the code is now compared with a version of itself that has been slipped one pulse time, for example 1011100, the same calculation is performed. The number of agreements is 3 and the number of disagreements is 4, leading to a correlation of -1. This is also shown in Table 2-1. After the code has been compared with a slipped version 7 times, the sequence repeats. The same is true for 3 identical codes in a row, i.e. the 3 fiber optic sensor system.

2.4 Code Correlation

Table 2-1 shows how timing slip affects autocorrelation. When the code is shifted by one or more bits, the correlation is -1. When the code is in the zero-shift condition, the correlation is 7. Sometimes these numbers are divided by the code length to normalize the maximum autocorrelation. Obviously normalization would lead to a zero-shift correlation of 1 and the shift correlation of -1/7 in this case.

Another important characteristic is cross correlation with other codes. A desirable property is for two codes to have low cross correlation no matter what the time difference is between them. This is necessary if one wants to send two codes without regard to timing and have the resultant signals have low crosstalk between them. An example of two 31 bit length codes that show low cross correlation regardless of timing slip is shown in Table 2-2. Here the maximum cross correlation is 7 whereas the maximum autocorrelation is 31. These codes could be used, without regard to timing, in a system together, unless the power of one was sufficiently larger than the other to cause a cross correlation close to the peak value.

2.5 Code Division Multiplexing of Fiber Optic Sensors

In an effort to network same-signal sensors using software and signal processing, Whitesel, *et al* [2.17] have demonstrated a system that multiplexes 32 fiber optic sensors using code division multiplexing, and information for much of this chapter is taken directly from that work. The operating schematic for this system is shown in Figure 2-3. Here, a master clock continuously puts out high frequency, on-off pulses into the code generator which changes these regularly occurring pulses into a seemingly irregular sequence of pulses m(t). The zero states (or zero crossings) occur at pseudorandom times that are some multiple of the pulse time, the period of the master clock. The code generator then drives a Light Emitting Diode (LED) thereby generating a pseudorandom optical pulse sequence transmitted through the 2 X M optical coupler to each of the M sensors. Each sensor is connected with slightly different lengths of fiber cable, causing the reflected signal from each Fabry-Perot sensor to each arrive at the receiver at slightly different times, as determined by the optical transit time through the different length cables. The 2 x M optical coupler divides the optical power to the point where the received signal, x(t), appears like random noise mixed with several versions of the transmitted pseudorandom pulse sequence. The sensor response at this point is not visually discernable. The averager enhances the sensor signals by reducing incoherent noise, generating an ensemble averaged signal g(t). The cross correlator calculates the correlation of the reflected sensor signals with the transmitted pseudorandom pulse sequence, $r_{mg}(\tau)$, which peaks in value when the time delay corresponds to the round trip optical transit time from the optical source to each optical sensor and back to the receiver. Noise that is not coherent to the transmitted pseudorandom pulse sequence is rejected. Each sensor peak occurs at a different point in time corresponding to the optical time delay in each sensor channel. The sensor signals are then displayed on the computer.

The cross correlation function, $r_{mg}(\tau)$, can be expressed as the sum of scaled and delayed versions of the autocorrelation function, $r_{mm}(\tau)$.

$$r_{mg}(\tau) = \int_{-\infty}^{+\infty} m(t) \cdot g(t+\tau) dt, \qquad 2.5.1$$

$$r_{mg}(\tau) = \int_{-\infty}^{+\infty} \{S_1[m(t) \cdot m(t-t_1+\tau)]\} + \{S_2[m(t) \cdot m(t-t_2+\tau)]\} + ... + \{S_M[m(t) \cdot m(t-t_M+\tau)]\} dt = \sum_{k=1}^{M} S_k \; r_{mm}(\tau - t_k), \qquad 2.5.2$$

where

S_k = Reflection coefficient from sensor k, (k = 1, 2,.....M),

m(t) = Transmitted pseudorandom pulse sequence,

g(t) = Ensemble averaged reflected signal from all sensors (based on 128 transmitted pseudorandom sequence pulses), and

t_k = Time delay for sensor k, (k = 1, 2,.....M) and τ = Lag-time variable.

The response of each sensor can then be determined by simply measuring the peak values of the calculated autocorrelation function at the appropriate delay times. However, there are residual errors that arise from cross coupling of the autocorrelation response of each sensor.

When there is no time delay match between the reflected pulses and the transmitted pulses, the autocorrelation function returns to a value of -1 times the sensor reflectivity, S_1, as shown in Figure 2-2(c). This is the residual value of the autocorrelation function and in general is given by $1/2^N$ for each sensor. For the 3 stage shift register shown in Figure 2-2(a) connected to 1 sensor, this residual value is 12.5%. Adding 2 more sensors for a total of three gives a residual error of $3/2^N$. In general the residual value of the autocorrelation function is given by $M/2^N$, Where M is the number of sensors. Three sensors with a 3 stage shift register gives a residual value of the autocorrelation function that increases to 3/8 of S_1, or 37.5%, as shown in Figure 2-2(d).

2.6 Summary of Code Division Multiplexing

Code division multiplexing of same-signal devices, here optical fiber sensors, has been successfully demonstrated. Key points of consideration are timing, slip, power budget, code length, autocorrelation, and cross correlation between two codes. The benefit of code division multiplexing as applied to optical fiber sensors is increased system signal to noise ratio thus allowing the multiplexing of a large number of sensors to one optical source [2.17]. With computing power continually decreasing in cost, code division multiplexing becomes more attractive since the complexity of the technique is inherently in the signal processing software as opposed to the optics. This means optical systems can be constructed without the manufacture of special optical devices which add cost.

This chapter has spelled out in detail the mathematics and algorithms behind code division multiplexing of a same-signal sensor source. These algorithms can be included in signal processing software to multiplex different type sensor signals. For this research we have chosen one of these to be Microelectromechanical Systems (MEMS) sensors.

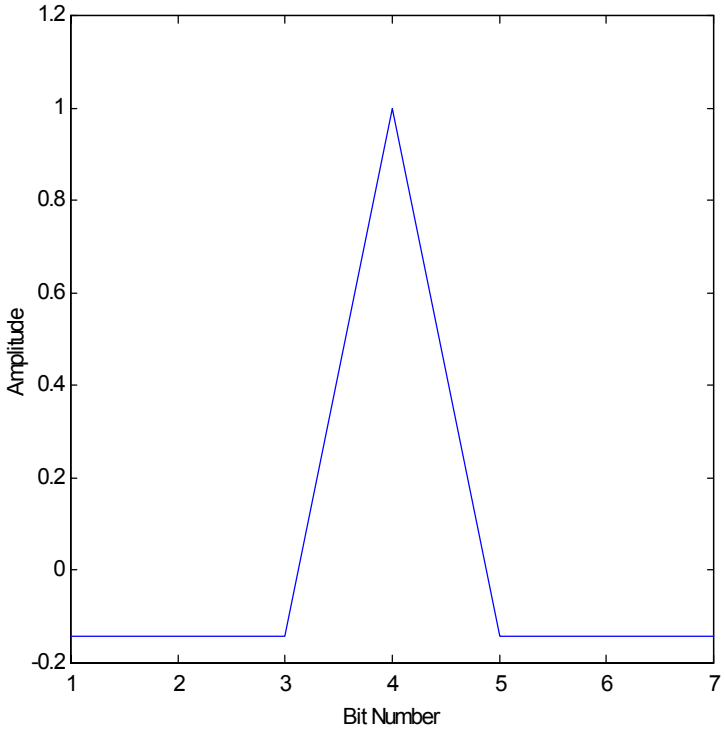

Figure 2-1. Autocorrelation function for a 7-bit sequence

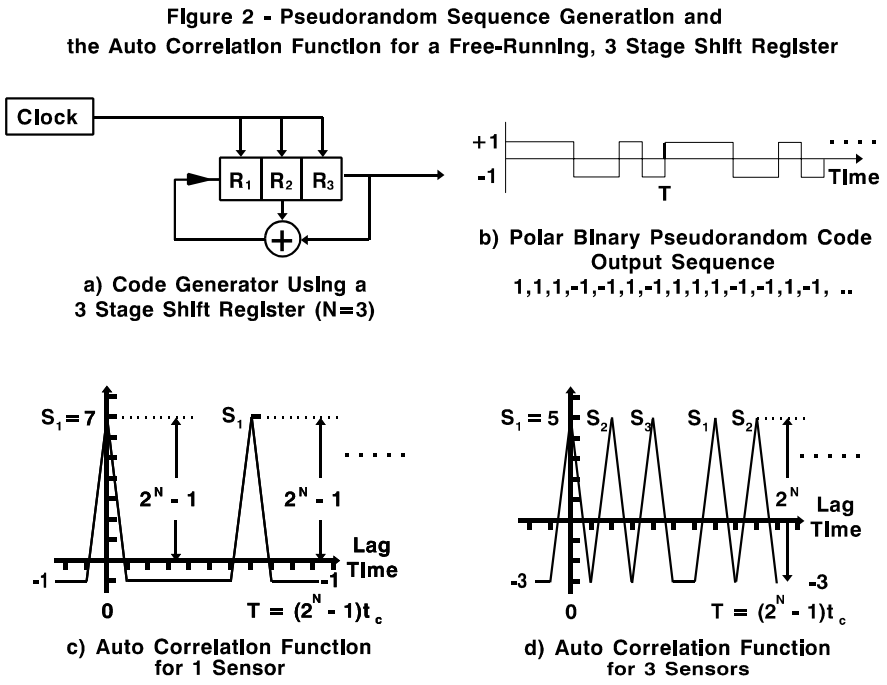

Figure 2-2 [2.17]. Pseudorandom sequence generation and autocorrelation for a 3-stage shift register

Shift	Sequence	Agreements (A)	Disagreements (D)	A-D
1	0111001	3	4	-1
2	1011100	3	4	-1
3	0101110	3	4	-1
4	0010111	3	4	-1
5	1001011	3	4	-1
6	1101001	3	4	-1
7	1110100	7	0	7

Table 2-1 [2.23]. Shift of a 7-bit sequence. Note that the correlation is -1 for all except the zero-shift condition where that correlation is 7

Shift	Agreements (A)	Disagreements (D)	A - D
0	15	16	-1
1	19	12	7
2	15	16	-1
3	11	20	-9
4	19	12	7
5	15	16	-1
6	19	12	7
7	15	16	-1
8	15	16	-1
9	15	16	-1
10	15	16	-1
11	19	12	7
12	19	12	7
13	15	16	-1
14	15	16	-1
15	19	12	7
16	15	26	-1
17	15	16	-1
18	11	20	-9
19	11	20	-9
20	11	20	-9
21	19	12	7
22	11	20	-9
23	15	16	-1
24	19	12	7
25	19	12	7
26	15	16	-1
27	15	16	-1
28	15	16	-1
29	15	16	-1
30	19	12	7
31	15	16	-1

Table 2-2 [2.23]. Correlation of two 31 bit length codes

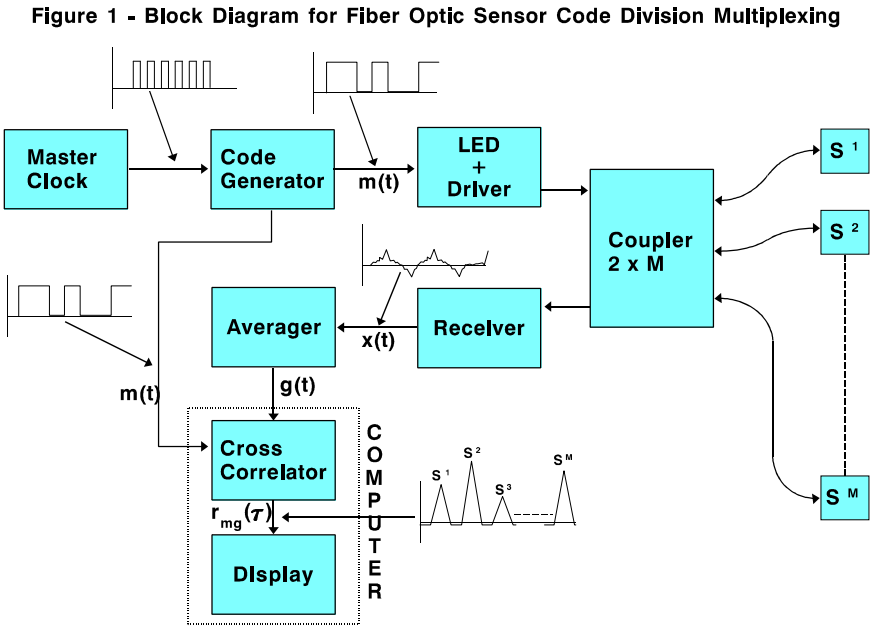

Figure 2-3 [2.17]. Operating schematic for a code division multiplexing system

Chapter 3 - MEMS Technology

3.1 MEMS Characteristics [3.1]

Even though this dissertation is concerned with the sensors that can be developed using MEMS technology, MEMS is much more than sensors. It is the manufacturing of a wide variety of items that are electronic and mechanical in nature. In addition to sensors, small motors, pumps, hydraulic systems, warhead fuses, high resolution displays, mass data storage devices are but a few of the devices that can be manufactured using MEMS technology.

The characteristics of MEMS fabrication are miniaturization, multiplicity, and microelectronics [3.1]. Miniaturization not only allows for small, lightweight devices, but these same devices have high resonant frequencies which mean higher operating frequencies and bandwidths for sensors and actuators. Multiplicity is the batch fabrication of MEMS and it makes the manufacture of large numbers of devices possible. Multiplicity also allows for flexibility in the design of massively-parallel, interconnected electromechanical systems. Microelectronics means simply that the electromechanical devices can be merged with microelectronics, thus allowing artificial intelligence and signal conditioning to be placed on a sensing device.

MEMS is a fabrication process, analogous to the integrated circuit fabrication process that has led to low- cost microelectronics circuits over the last thirty years. With MEMS, the process is that of combining microelectronics with mechanical and electro-mechanical devices. All of these items can be mounted on a single substrate.

A lot of what MEMS is today is due to the large infusion of capital from the Defense Advanced Research Projects Agency (DARPA). In this program millions of dollars have been put into developing MEMS devices and the MEMS infrastructure. Now small, lightweight devices are being manufactured for applications that include medical, military, and civilian.

3.2 MEMS Fabrication and Integrated circuits [3.2]

The MEMS fabrication process consists of putting down layers of different materials onto a silicon substrate then, using masks and etching material, etching some of the layers away to form components. This process is the one used by MCNC (formerly the Microelectronics Center of North Carolina, the acronym is now the official name) which is one of the facilities that is a result of the DARPA funding.

3.3 MEMS Integrated Circuits

Electronic components can be put on the substrate using the same procedure whenever practical. However it is sometimes better to procure a separate integrated circuit and attach it to the silicon substrate. The advantage of using a separate chip are lower cost and reduction of the effects of heat and vibration on the electronics. An example of this process is the MCNC "flip chip" where the integrated circuit chip is attached to the electro mechanical chip using solder bumps. With this process, one has an integrated chip package that consists of both electronics and electromechanical devices. Illustrations of a MEMS integrated circuit assembly are shown in Figures 3-1 and 3-2 [3-3].

3.4 MEMS Sensor Applications

While a multitude of devices can be manufactured using MEMS fabrication technology, it is sensors that have the highest application. The market for sensors in the United States is primarily the automotive industry. There are plans for MEMS sensors that measure pressure and temperature in the engine compartments of automobiles and also so called "smart sensors" where the tire pressure is measured and then transmitted to a control panel to warn truck drivers of a tire that is under inflated. MEMS sensors are becoming more popular with different applications such as refrigeration system parameter detection, isopropyl alcohol detection, guidance systems, anti-braking systems, gyroscopes, and aircraft wing monitoring [3.1].

3.5 A Commercial MEMS Sensor

By far the most advanced MEMS sensor application to date is the Analog Devices ADXL-50 acceleration sensor and its "little brother" the ADXL-05 sensor. The first measures 50 g's full scale while the second measures 5 g's full scale [3.3, 3.4]. The ADXL-50 is used in automobile air bags for deployment upon vehicle impact. Both of these sensors contain a capacitive sensor and an electronics package of over 200 transistors on the same silicon chip.

The ADXL05 will measure from a full-scale range of plus or minus 5 g's to plus or minus 1 g or less, has a noise floor of 500 ug/ root Hz which allows signals below 5 mill-g to be resolved. The accelerometer will measure both AC and DC vibration [3.4]. A view of the sensor "wafer" is shown in Figure 3-3 [3.5]. Here it can be seen that the sensor consists of the sensing element shown in the approximate center of the figure and the various electronics components.

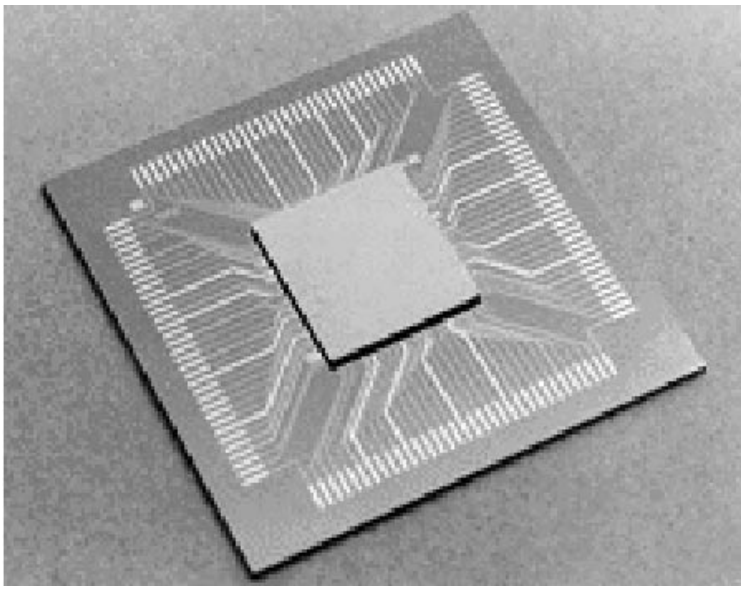

Figure 3-1 [3.3]. Photograph of MEMS device and IC mounted together.

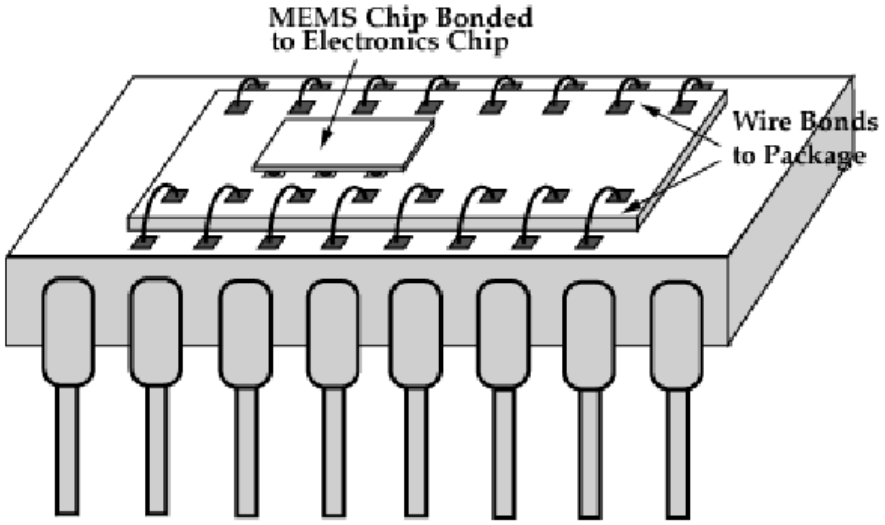

Figure 3-2 [3.3]. MEMS and IC chip mounted on a substrate with leads.

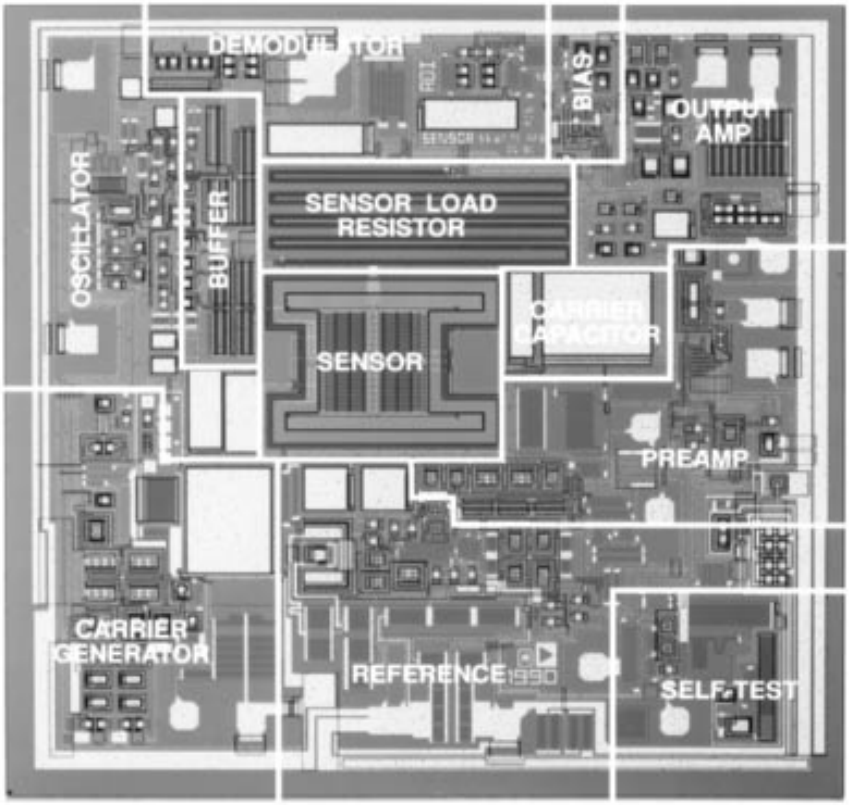

Analog Devices' ADXL-50, the industry's first surface micromachined accelerometer, includes signal conditioning on chip.

Figure 3-3 [3.5]. Analog Devices Accelerometer.

Chapter 4 - Systems Analysis and Design

4.1 Description

The central goal of the work was multiplexing different sensor signal sources using a software and signal processing approach. An analysis was performed to determine the issues involved in multiplexing the different sensor signal sources, and how those issues could be resolved using good software design. The systems analysis also determined the correct operating parameters.

A schematic of the effort is shown in Figure 4-1. There are two code generators, one for the subsystem of fiber optic sensors, and one for the simulated MEMS sensor. These sensors generate different codes so the MEMS sensor can send information without regard to the timing of the fiber optic sensors and vice versa. The optical signals from the MEMS and fiber optic sensors are fed through couplers into the receiver where they are converted to electrical signals and then fed into the computer. There the cross correlation is taken and the measurand computed and displayed.

The simulated MEMS sensor consists of a commercially available accelerometer, the Analog Devices ADXL-05, described in Chapter 3, which is identical to the ADXL-50 air bag sensor, but has a lower operating range of approximately 5 g's as opposed to the ADXL-50's 50 g range [3.3, 3.4]. This sensor modulates an LED with a 0 to 5 volt output which is pulsed by the pseudo random bit generator. This was the manner in which the MEMS sensor was used to simulate the second type of sensor after fiber optics sensor. Other components were chosen to ensure the system was compatible with the overall goal of multiplexing different sensors signal sources.

The components selected for the system include the Hewlett Packard 1414T LED and the companion 2416T detector . The optical fiber selected was 62.5/125 um multimode graded index

and the couplers were Gould 2x2 with approximately 4db overall insertion loss. These components were chosen due to their availability and relatively low cost.

4.2 Power Budget

In order for the system to operate with compatibility of the two different sensor types, a power budget was performed which is shown below. Referring to Figure 4-1, the system is divided into two sections, A and B, and then analyzed for the power budget.

SECTION A:

The parameters are LED output: -11dBm, total coupler insertion loss 4dB each, connector loss 1 dB each. Taking the case of the fiber optic intensity sensors first and going from the LED to the detector, the power budget calculation is:

$$P_{FO} - 1 - 4 - 4 - 4 - 1 = P_{FO} - 14\ dB_m \text{ at the detector}$$

SECTION B:
Going from the LED in the simulated MEMS sensor, we have:

$$P_{MEMS} - 1 - 4 - 1 = P_{MEMS} - 6\ dB_m$$

From this, in order to have signals of approximately equal power at the detector,

$$P_{FO} = P_{MEMS} - 8\ dBm$$

This means that the power in the fiber optic sensor LED must be 8 db higher than the power in the MEMS LED. This can be accomplished by correct circuit design.

4.3 Correlation

In order to allow both types of sensors to send and receive signals on the same transmission path, the issue of using software to determine signal correlation was studied. The study found that a major issue in code division multiplexing as applied to fiber optic and MEMS sensors is calculating the cross correlation of two signals. While the calculation can be performed in the time domain, the total number of calculations can be rather high. What is desired is an expression of the cross correlation in the frequency domain. Performing the cross correlation in the time domain takes approximately N^2 calculations where N is the code length, and performing the entire calculation in the frequency domain requires approximately $3N\log_2(N)$ calculations. [4.1]. The expression for the time domain calculation of the cross correlation of two signals is derived below [4.2].

The cross correlation function $r_{fg}(\tau)$ is defined as

$$r_{fg}(\tau) = \int_{-\infty}^{\infty} f(t)g(t+\tau)dt. \qquad 4.3.1$$

Taking the Fourier transform of equation 4.3.1 we obtain

$$F(r_{fg}(\tau)) = \int_{-\infty}^{\infty}\int_{-\infty}^{\infty} f(t)\, g(t+\tau)\, dt\ e^{-j\omega\tau} d\tau. \qquad 4.3.2$$

Interchanging the order of integration in equation 4.3.2 we have

$$F(r_{fg}(\tau)) = \int_{-\infty}^{\infty} f(t) \int_{-\infty}^{\infty} g(t+\tau)\ e^{-j\omega\tau}\, d\tau\, dt. \qquad 4.3.3$$

Use of the time delay property gives

$$F(r_{fg}(\tau)) = \int_{-\infty}^{\infty} f(t)\, G(\omega)\ e^{-j\omega t}\, dt, \qquad 4.3.4$$

and finally, using the definition of the Fourier transform, we have

$$F(r_{fg}(\tau)) = F(\omega)\, G(\omega). \qquad 4.3.5$$

From this we can see that the cross correlation is simply the inverse Fourier transform of the products of the Fourier transforms of both the transmitted and returned signal. Thus we have obtained the necessary expression to allow efficient software to be developed for the signal processing.

4.4 Code Timing

Not only is it necessary to have different types of sensors signals multiplexed together, it is also necessary to have the same type of sensors multiplexed onto the system. Here the fiber optic sensors need to have a delay in order for the software to be able to separate out the signals. To obtain different codes for each sensor, two code generators were used, one for the fiber optic sensors and one for the simulated MEMS sensor. Since the fiber optic sensors are in the same line, the output of fiber optic sensor 1 can be discerned from that of fiber optic sensor 2 simply by putting in the delay coil shown in Figure 4-1. If the length of this delay coil is adjusted to

make the delay greater than one pulse time, the outputs of both sensors can be detected using the original code.

$$s = vt, \tag{4.4.1}$$

$$v = \frac{c}{n}, \tag{4.4.2}$$

$$s = \frac{ct}{n}, \tag{4.4.3}$$

where c = $3(10^8)$ meters per second, n = index of refraction in the fiber core = 1.468, and t = 1 pulse time = 1/frequency = 1/1.8432Mhz. From this we obtain

$$s = \frac{3(10^8)}{1.468}\ \frac{1}{1.8432(10^6)} = 111\ meters.$$

Therefore we need a delay coil of at least 111 meters in length to provide the new code. Thus we are able to create a physical design that allows for correct code timing of the two fiber optic sensors and also allows for the signal processing to separate them.

4.5. Code Selection

In this mixed-signal system it is necessary to allow all types of sensors to be received, and this is where code selection comes into play. If the correct codes are not implemented in the software design, the system will not work. In view of this, a detailed analysis of all possible codes was undertaken. A systems analysis was performed to determine the proper codes to use and to

predict the experimental results. A MATLAB computer program was written to generate code pairs and their correlation plots, and to generate theoretical code pulses and correlation functions.

Code selection is extremely important. The best codes to use are those that have already been determined to have characteristics attractive to signal processing [2.23]. It is desired to have pairs of codes that have a high degree of autocorrelation and a low degree of cross correlation, and certain codes lend themselves to this application because they have these properties.

For ease of experimentation, a code length of 127 bits was chosen. All maximal bit length codes of this length were compared to determine the low cross correlation. The results are shown in Figures 4-2 through 4-19. As can be seen, the lowest cross correlation was -17 and this was for several code pairs. Code taps of 7 1 and 7 3 were chosen in order to facilitate the experimentation. The correlation shows that both signals can be discerned, even though they are from different sensor sources.

4.6. Predicted Results

A MATLAB computer program was written to predict the actual results. These are illustrated in Figures 4-20 through 4-23. The output of a 127 bit length code is shown in Figure 4-20. This is the code that is sent out from either fiber optic or MEMS sensor. Figure 4-21 shows the same code after noise is added. This simulates the code received at the detector. Figure 4-22 shows the 7 1 and 7 3 codes after correlation. Figure 4-23 shows the 7 1 received code correlated with another 7 1 code. Note the correlation peak on the left hand side. The correlation is quite discernible to the naked eye, whereas the correlation between the 7 1 and 7 3 codes does not reveal any peak. This is desirable since crosstalk between the fiber optic and MEMS sensors should be kept as low as possible.

4.7. Summary of the Systems Analysis and Design

In designing the software package, the MATLAB computer program was used because it possesses sophisticated signal processing capabilities necessary for a mixed signal sensors system. The signal processing used filters out the noise and the unwanted sensor signals to allow one to discern the desired sensor signal.

Some issues that were uncovered were how to keep the signals separate and how to transform the sensor output of one system into an ouput that is compatible with the other system. Further, one could combine signals with a simple time domain or wavelength division method, but these would limit the number of possible maximum number of sensors since there is no inherent gain in these methods. That is why code division mutilpexing was chosen.

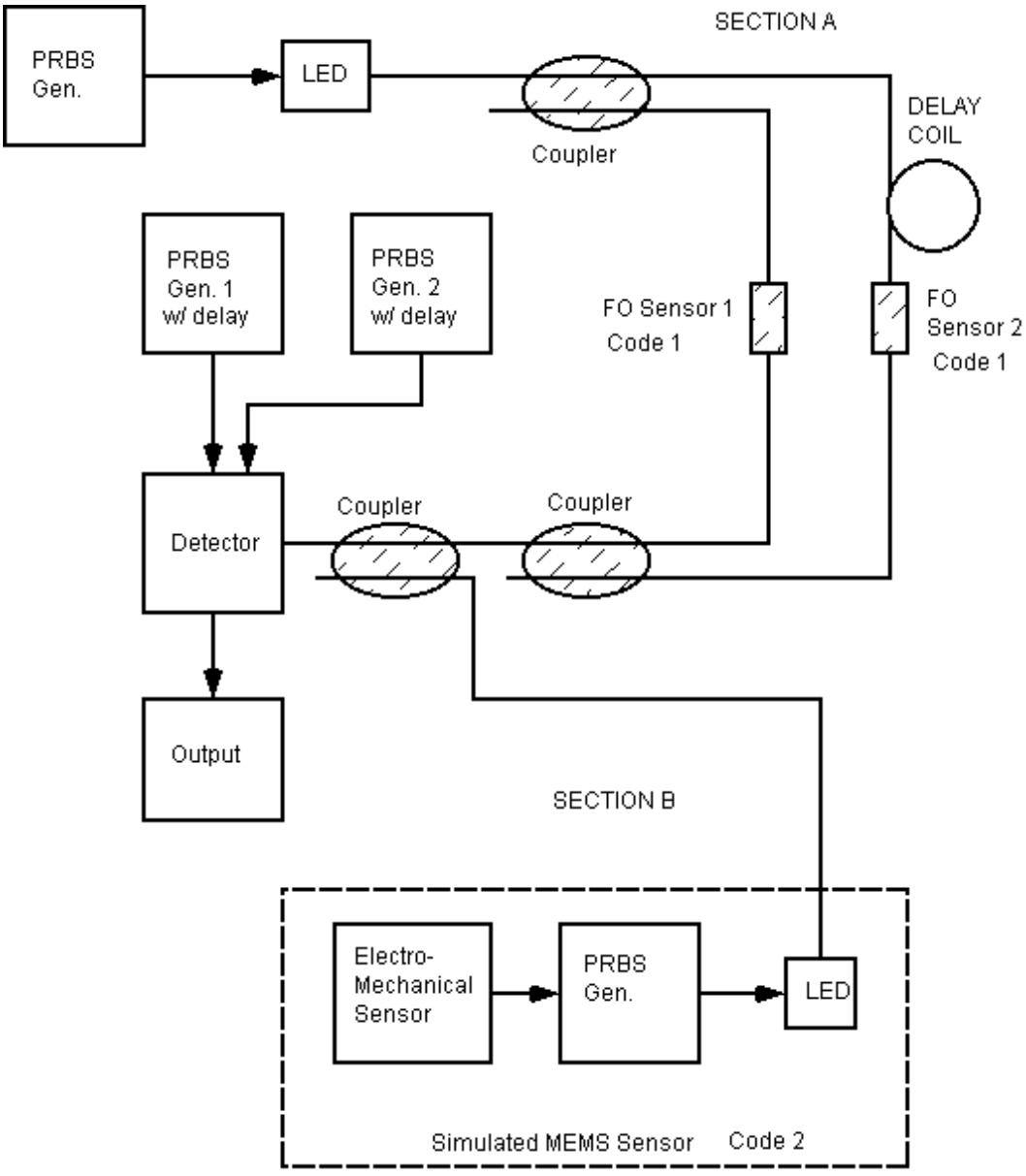

Figure 4-1. The CDM network consisting of two fiber optic and one MEMS sensor

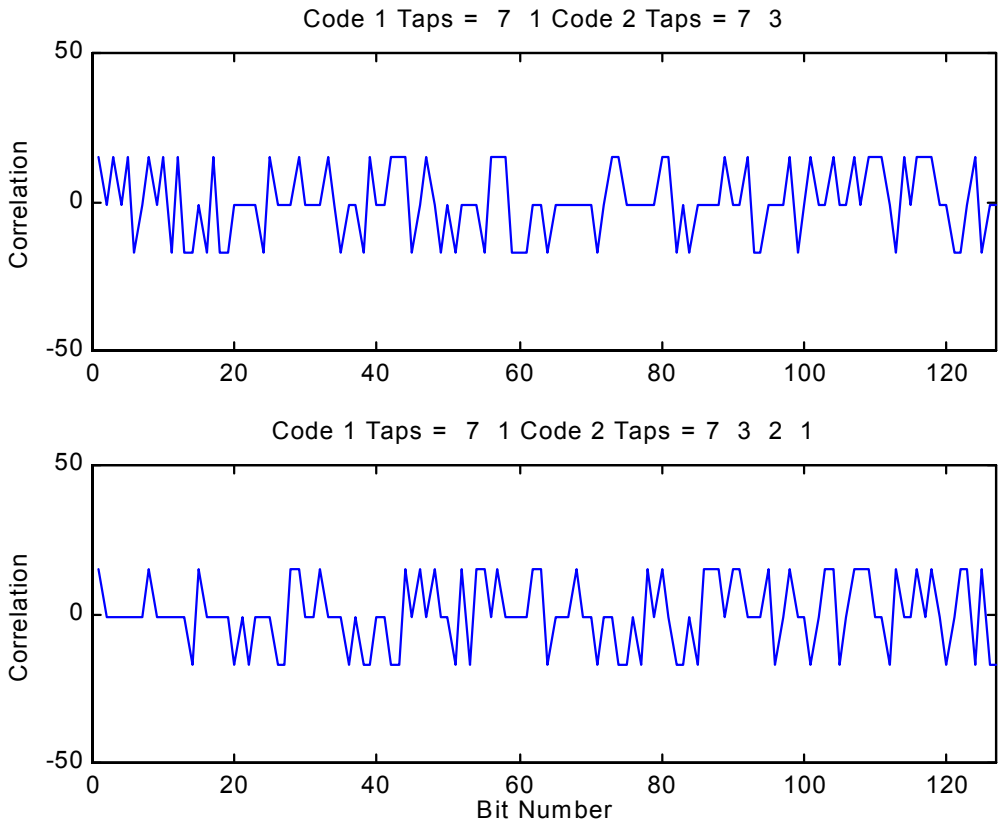

Figure 4-2. Correlations of Code Pairs 7 1, 7 3 and 7 1, 7 3 2 1.

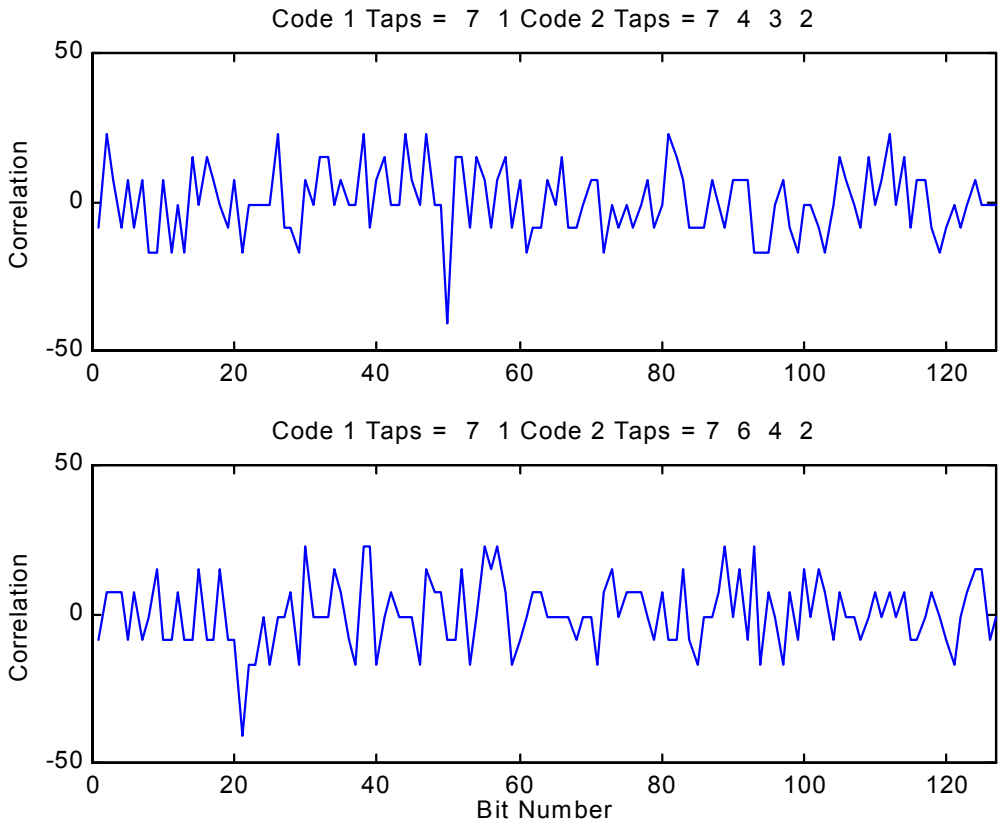

Figure 4-3. Correlations of Code Pairs 7 1, 7 4 3 2 and 7 1, 7 6 4 2 .

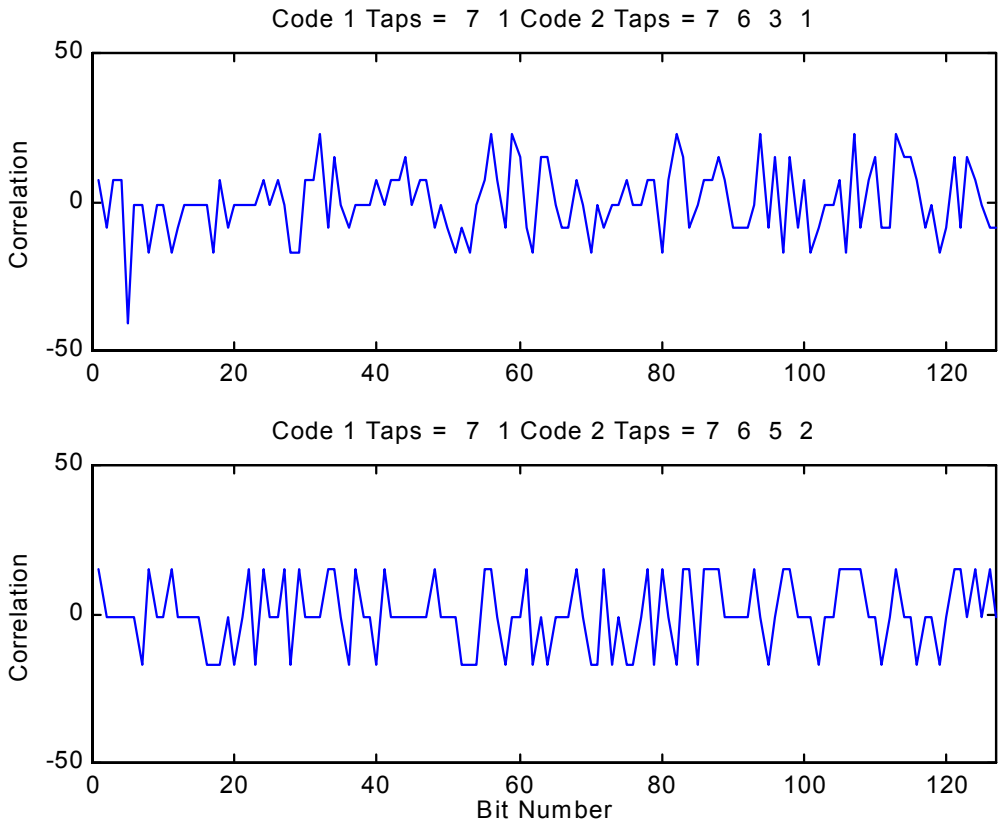

Figure 4-4. Correlations of Code Pairs 7 1, 7 6 3 1 and 7 1, 7 6 5 2 .

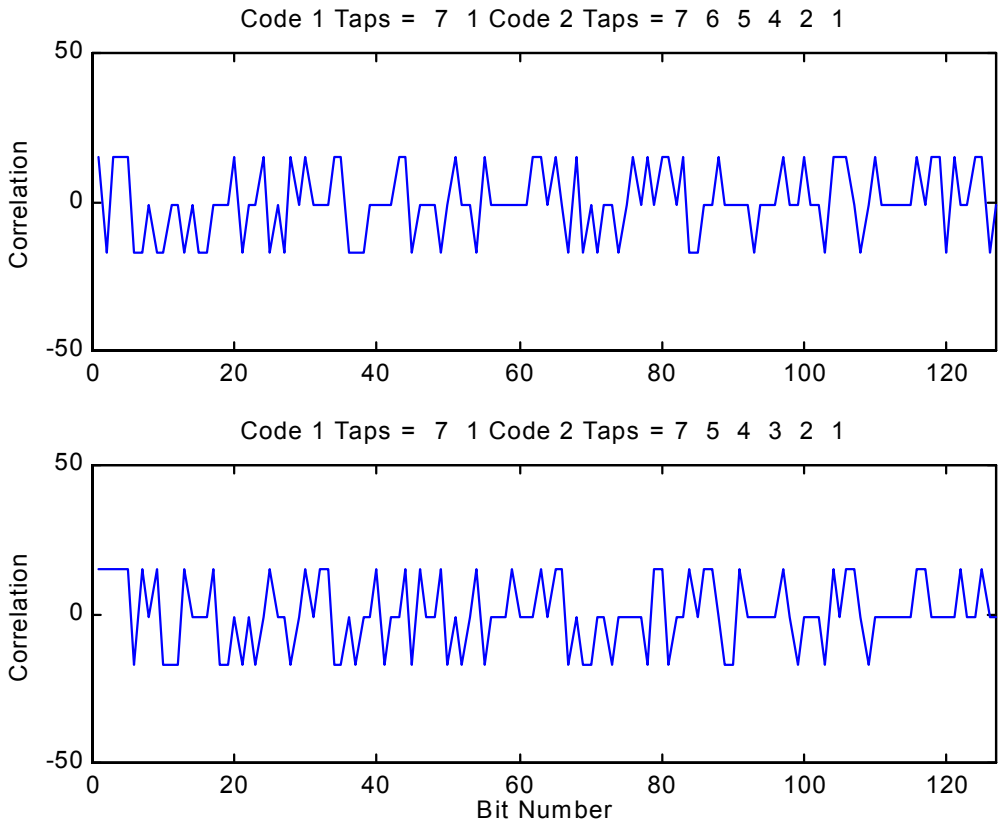

Figure 4-5. Correlations of Code Pairs 7 1, 7 6 5 4 2 1 and 7 1, 7 5 4 3 2 1.

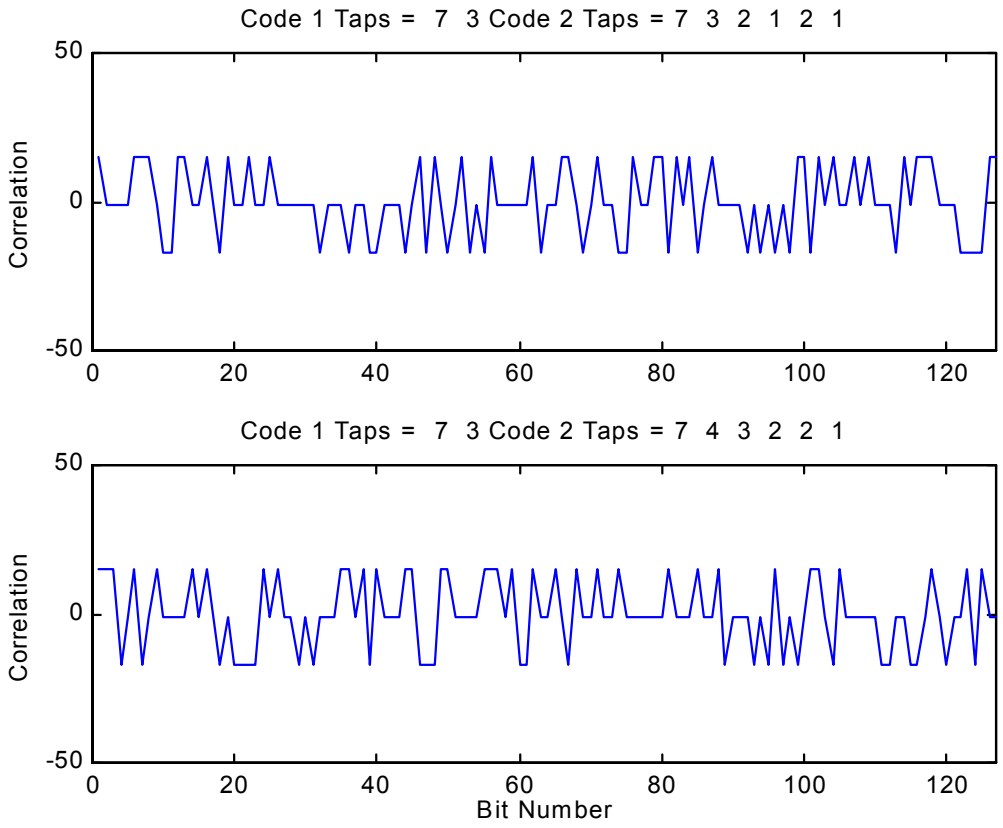

Figure 4-6. Correlations of Code Pairs 7 3, 7 3 2 1 and 7 3, 7 4 3 2 1.

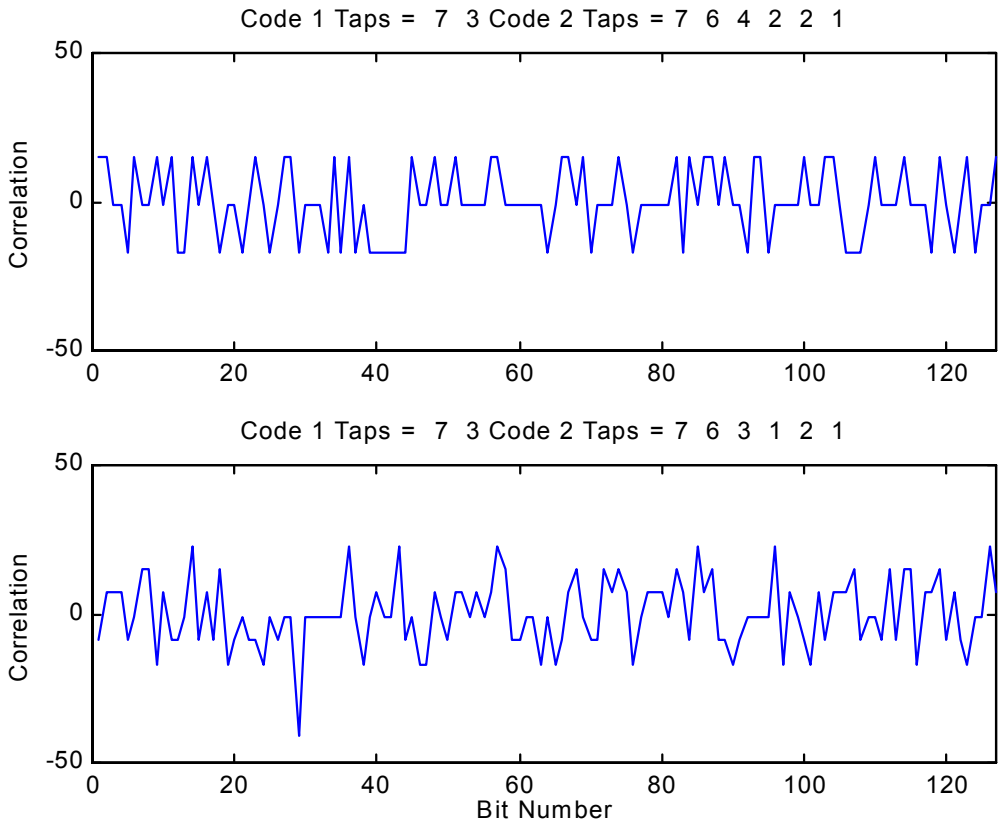

Figure 4-7. Correlations of Code Pairs 7 6, 7 6 4 2 1 and 7 6, 7 6 3 2 1.

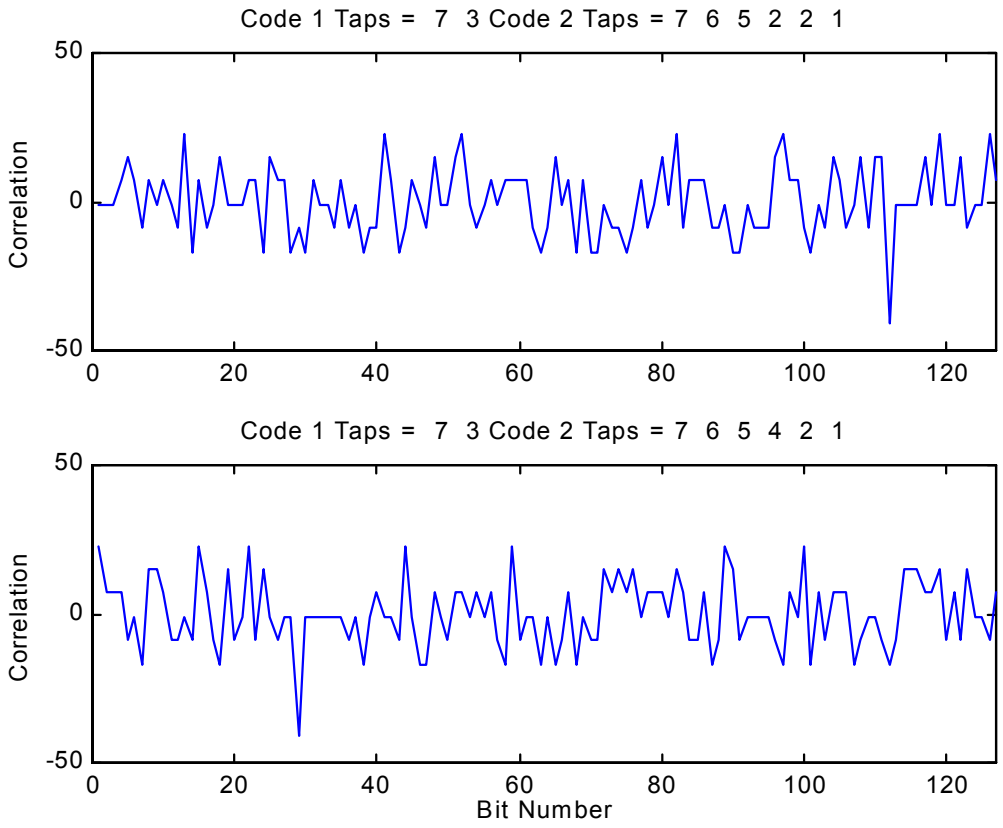

Figure 4-8. Correlations of Code Pairs 7 3, 7 6 2 1 and 7 3, 7 6 5 4 2 1.

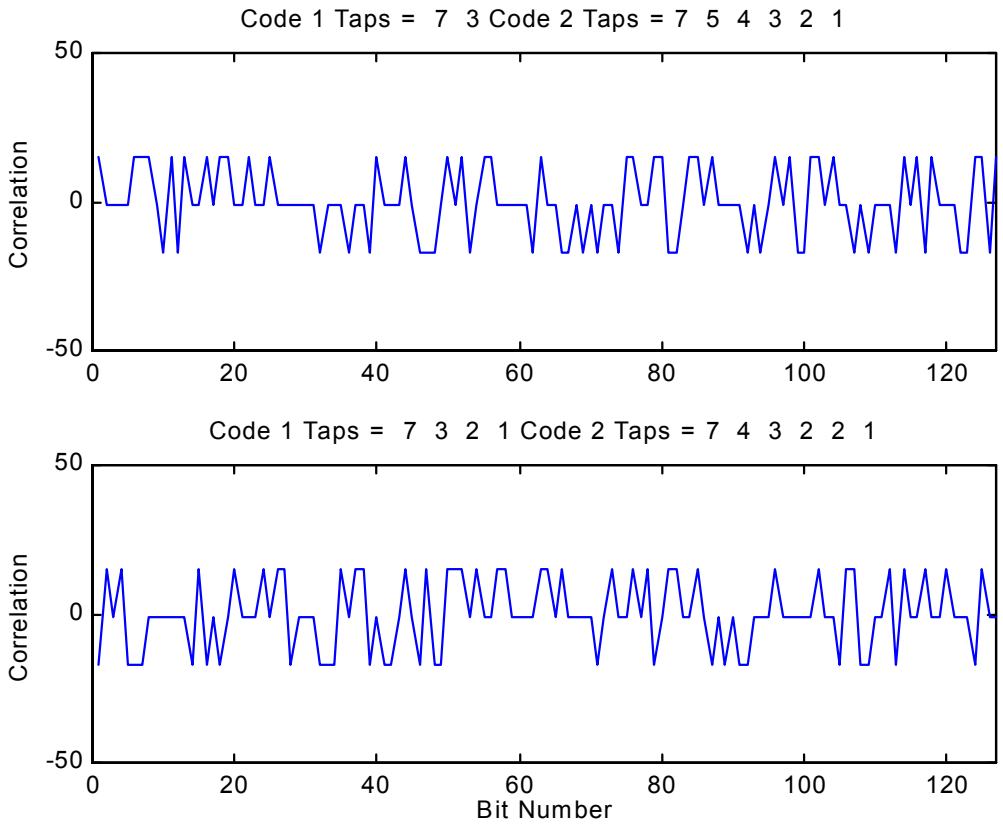

Figure 4-9. Correlations of Code Pairs 7 3, 7 5 4 3 2 1 and 7 3, 7 4 3 2 1.

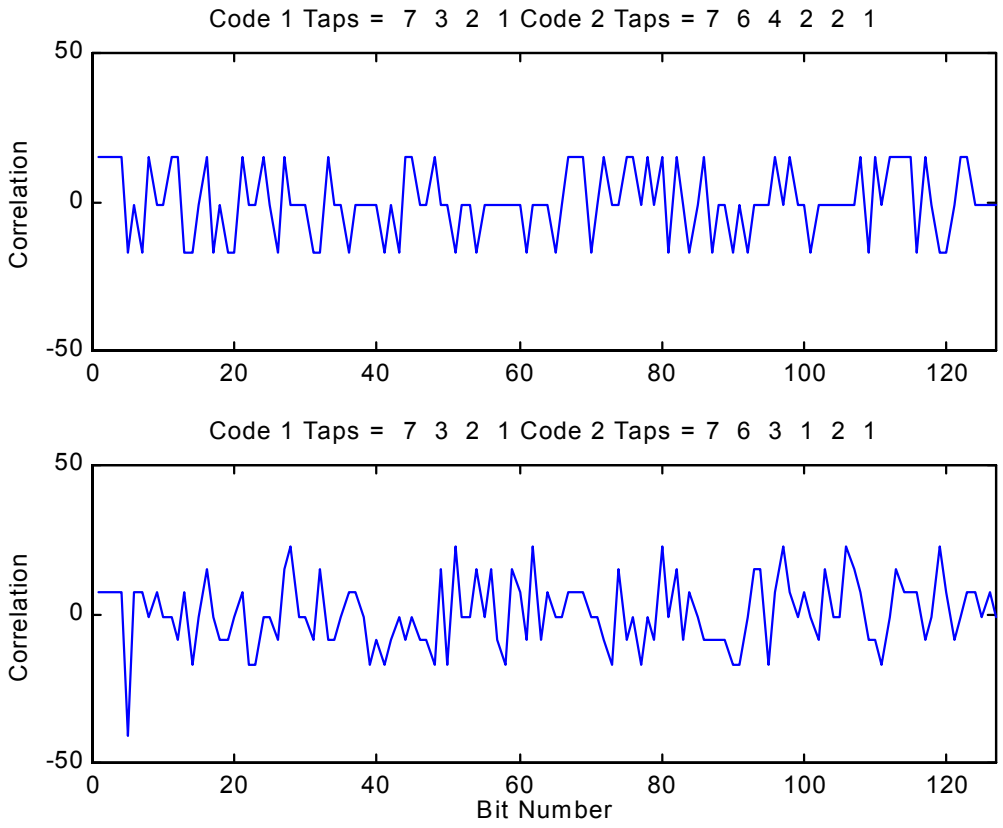

Figure 4-10. Correlations of Code Pairs 7 3 2 1, 7 6 4 2 1 and 7 3 2 1, 7 6 3 2 1.

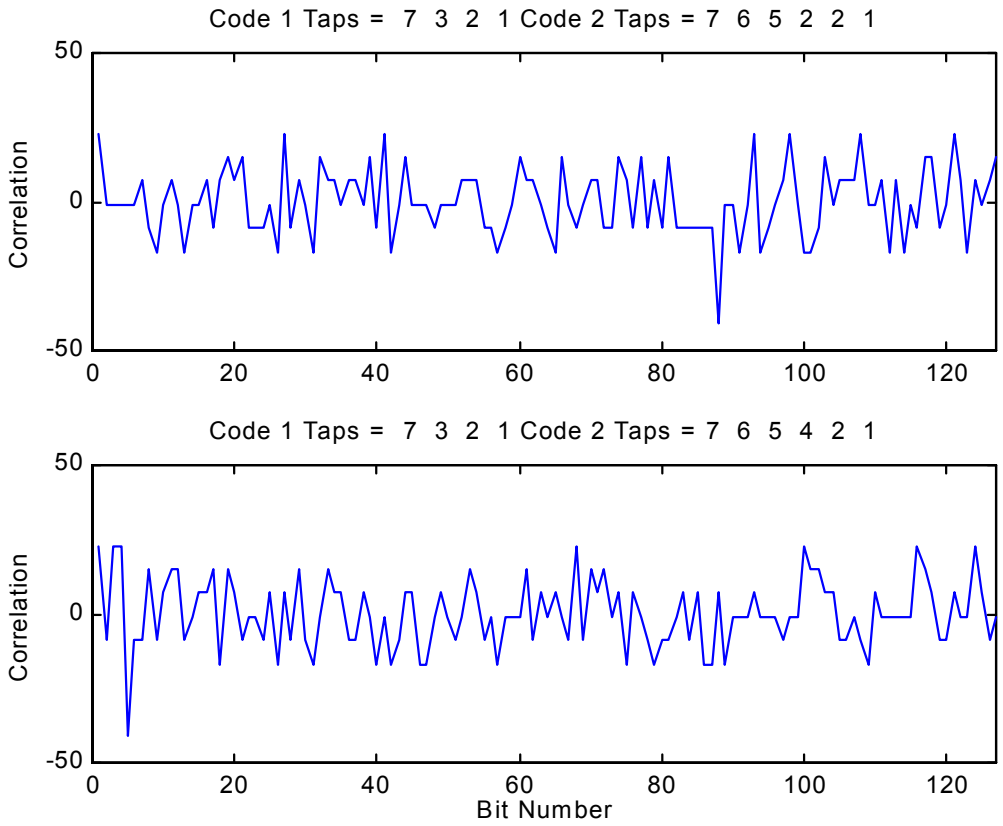

Figure 4-11. Correlations of Code Pairs 7 3 2 1, 7 3 2 1 and 7 3 2 1, 7 6 5 4 2 1.

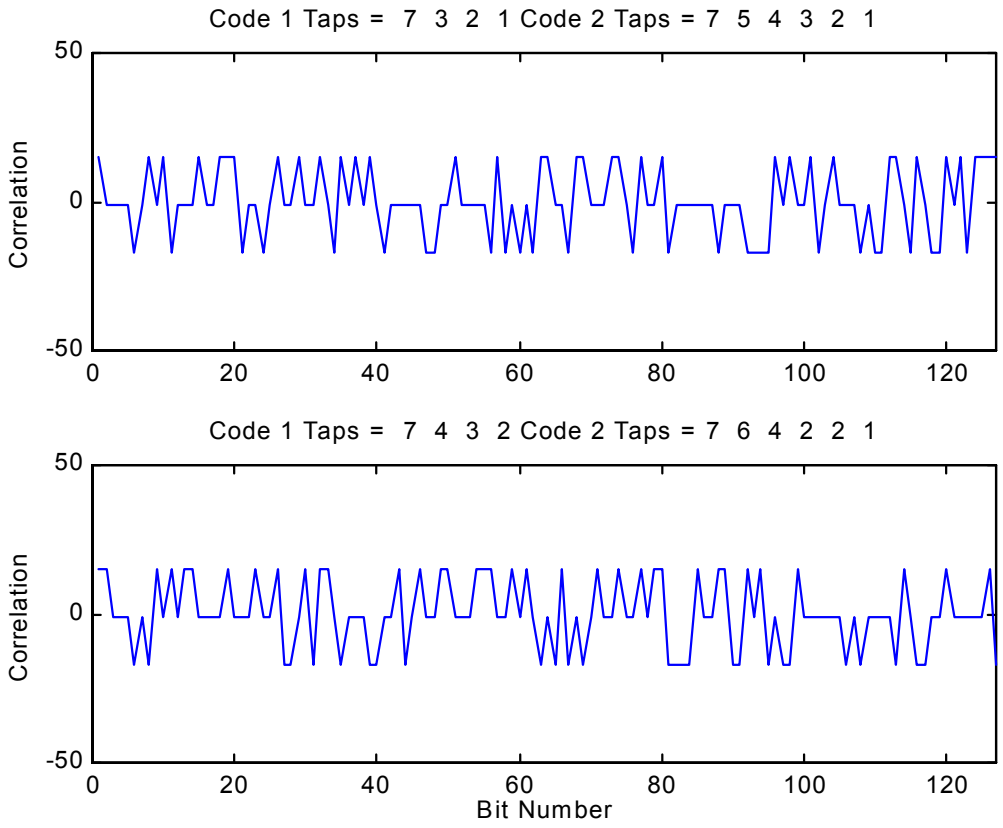

Figure 4-12. Correlations of Code Pairs 7 3 2 1, 7 5 4 3 2 1 and 7 4 3 2, 7 6 4 2 1.

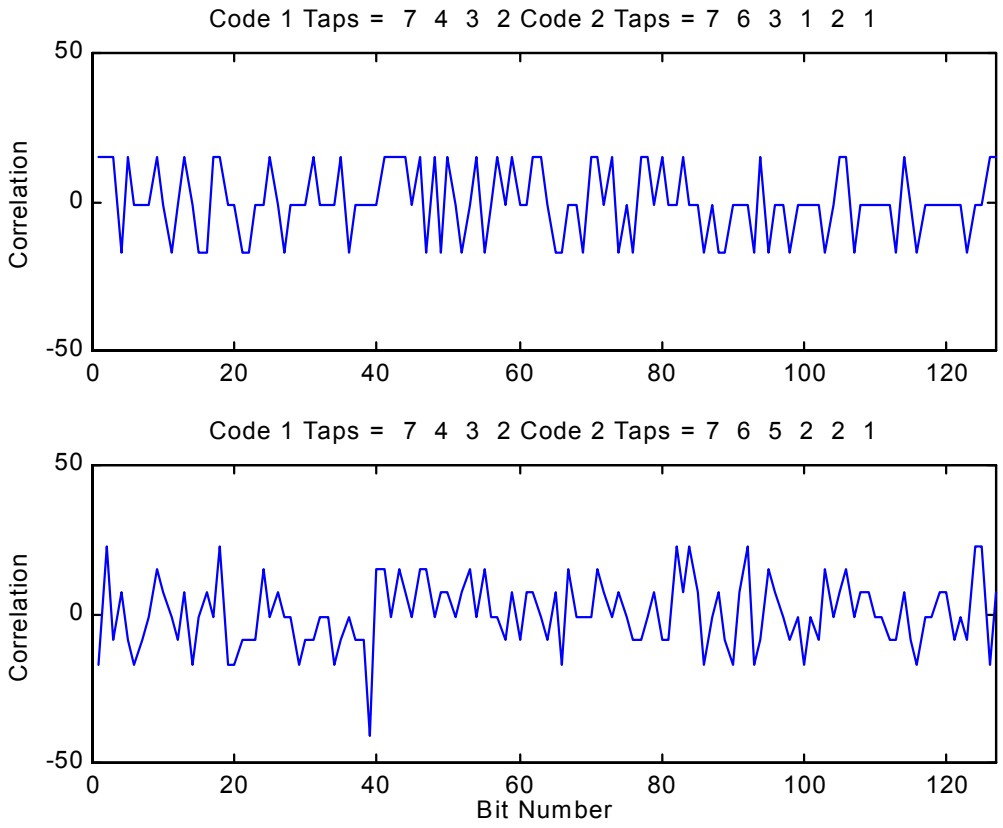

Figure 4-13. Correlations of Code Pairs 7 4 3 2, 7 6 3 2 1 and 7 4 3 2, 7 6 2 1.

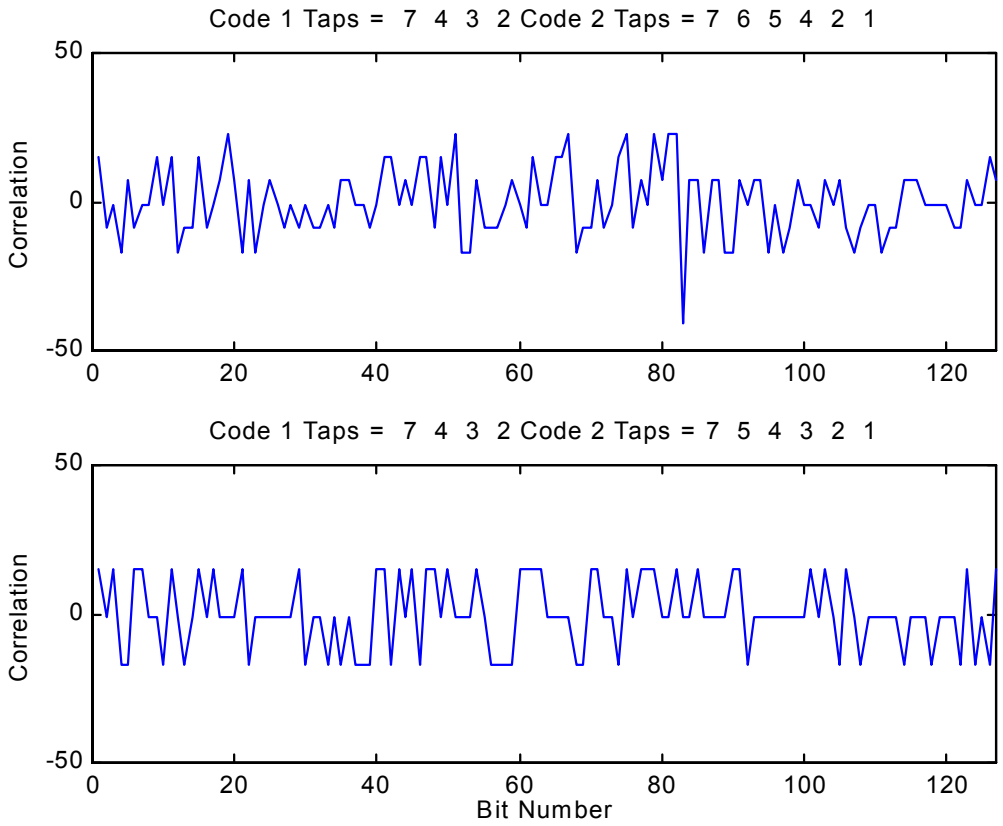

Figure 4-14. Correlations of Code Pairs 7 4 3 2, 7 6 4 2 1 and 7 4 3 2, 7 5 4 3 2 1.

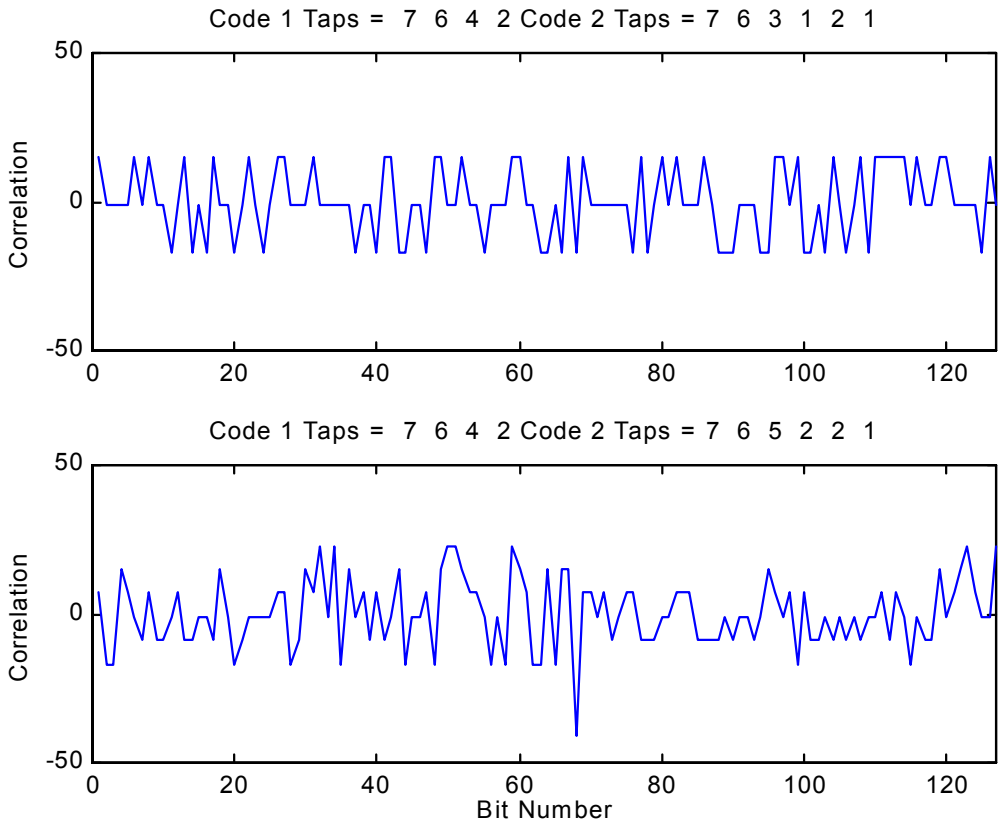

Figure 4-15. Correlations of Code Pairs 7 6 4 2, 7 6 3 2 1 and 7 6 4 2, 7 6 2 1.

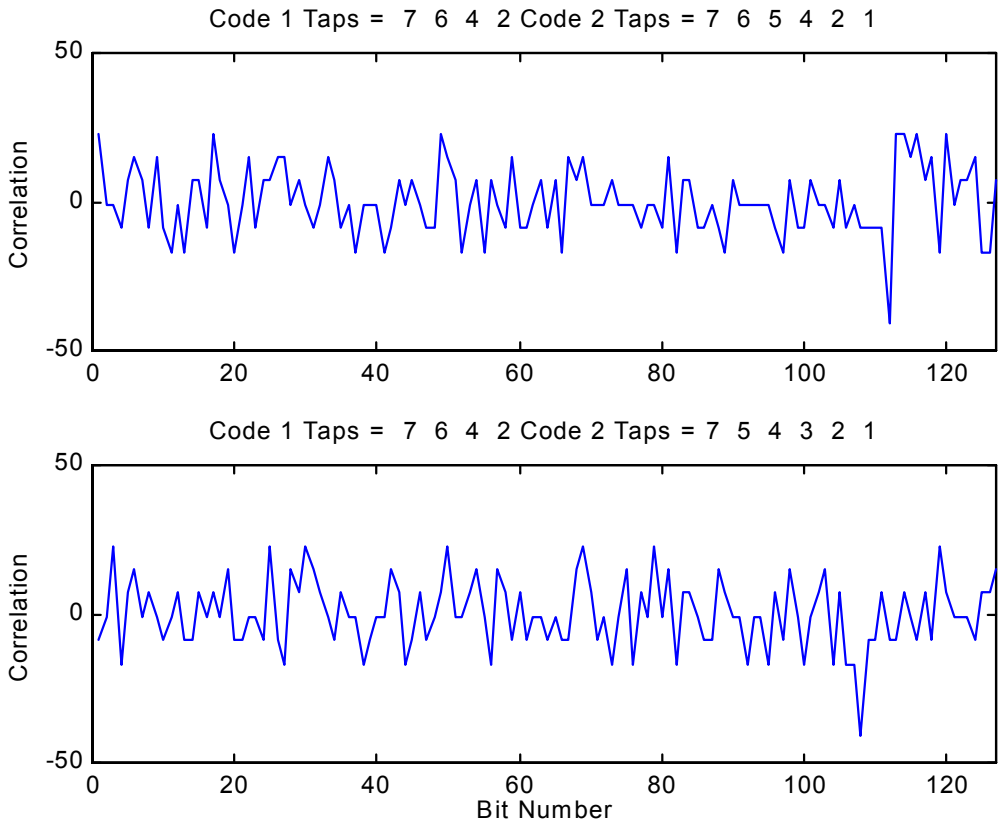

Figure 4-16. Correlations of Code Pairs 7 6 4 2, 7 6 5 4 2 1 and 7 6 4 2, 7 5 4 3 2 1.

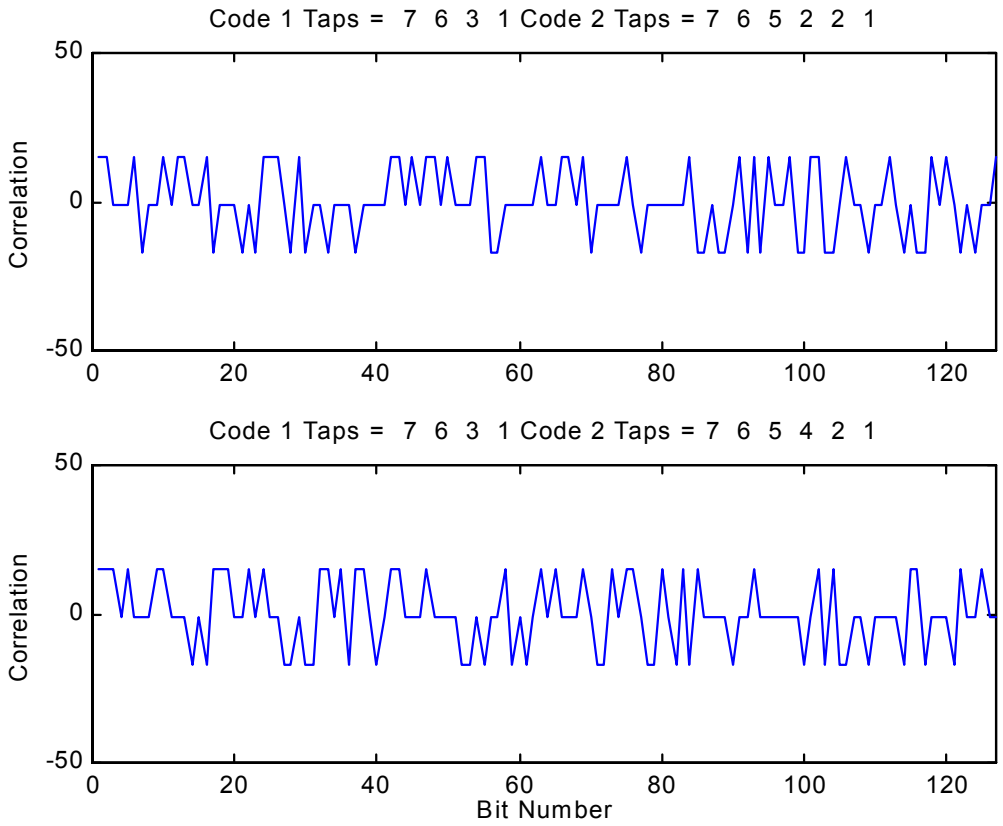

Figure 4-17. Correlations of Code Pairs 7 6 3 1 ,7 6 5 2 1 and 7 6 3 1, 7 6 5 4 2 1.

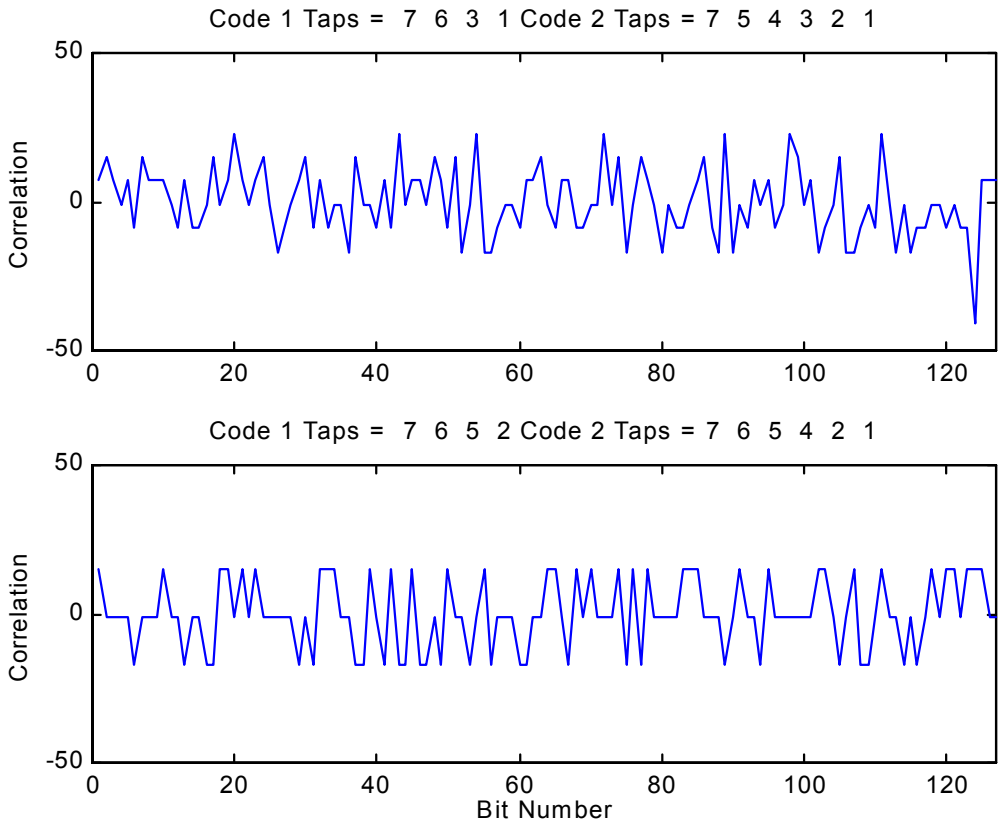

Figure 4-18. Correlations of Code Pairs 7 6 3 1, 7 5 4 3 2 1 and 7 6 5 2, 7 6 5 4 2 1.

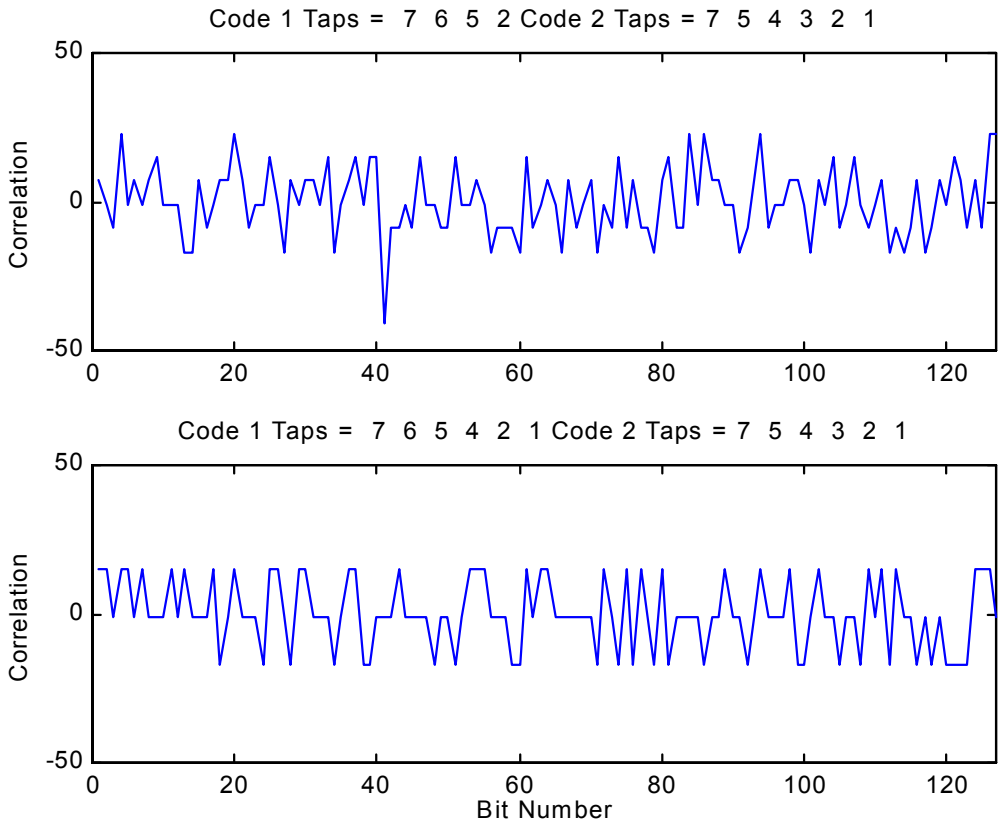

Figure 4-19. Correlations of Code Pairs 7 6 5 2, 7 5 4 3 2 1 and 7 6 5 4 2 1, 7 5 4 3 2 1.

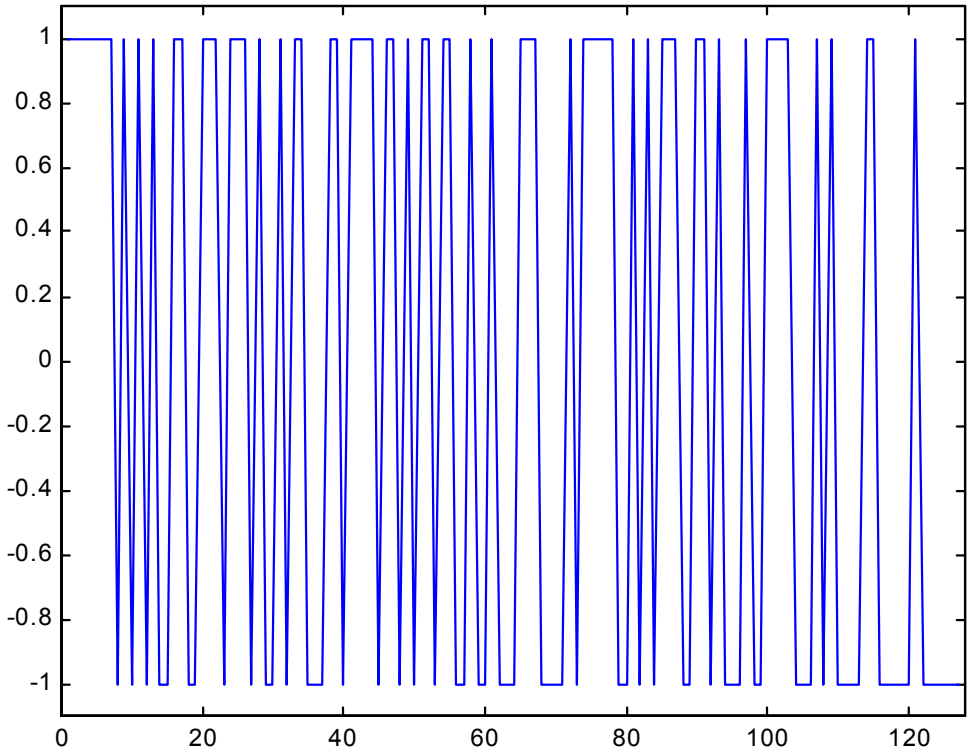

Figure 4-20. Code with taps 7 1, no noise.

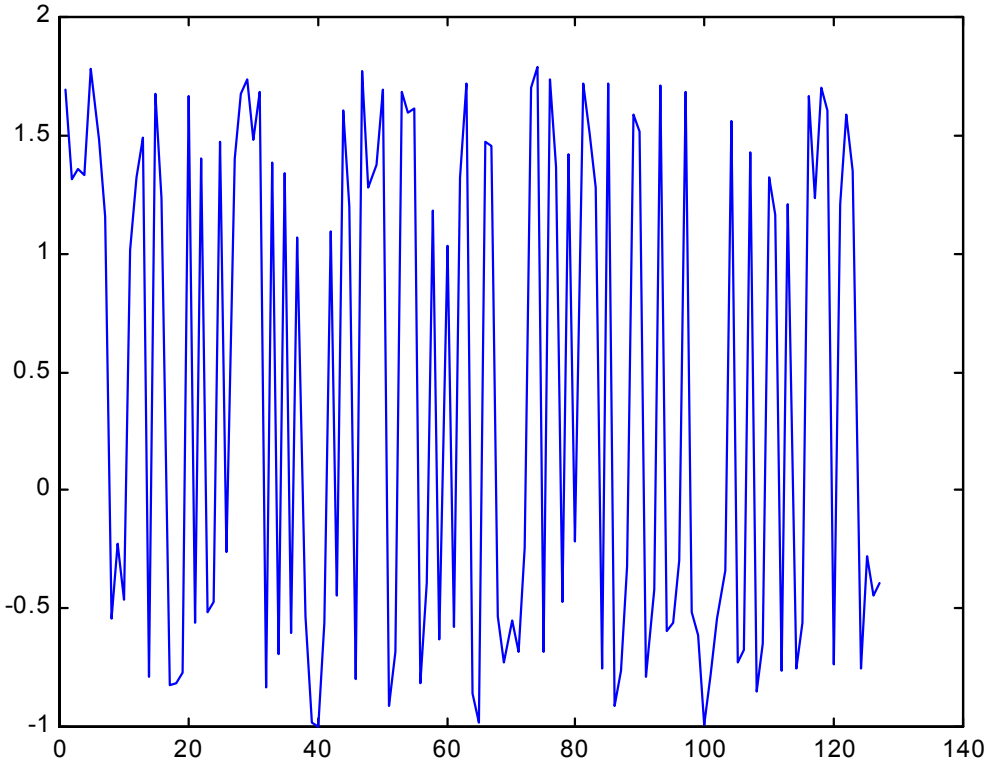

Figure 4-21. Code with taps 7 1, noise added.

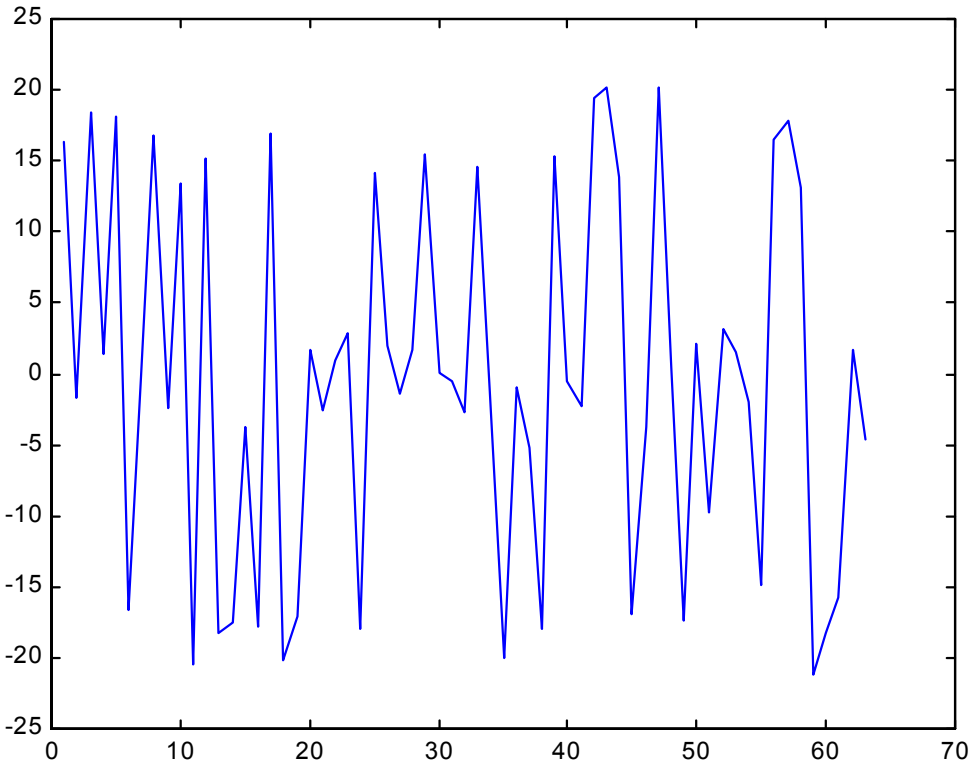

Figure 4-22. Code with taps at 7 1, noise added correlated with code with taps at 7 3.

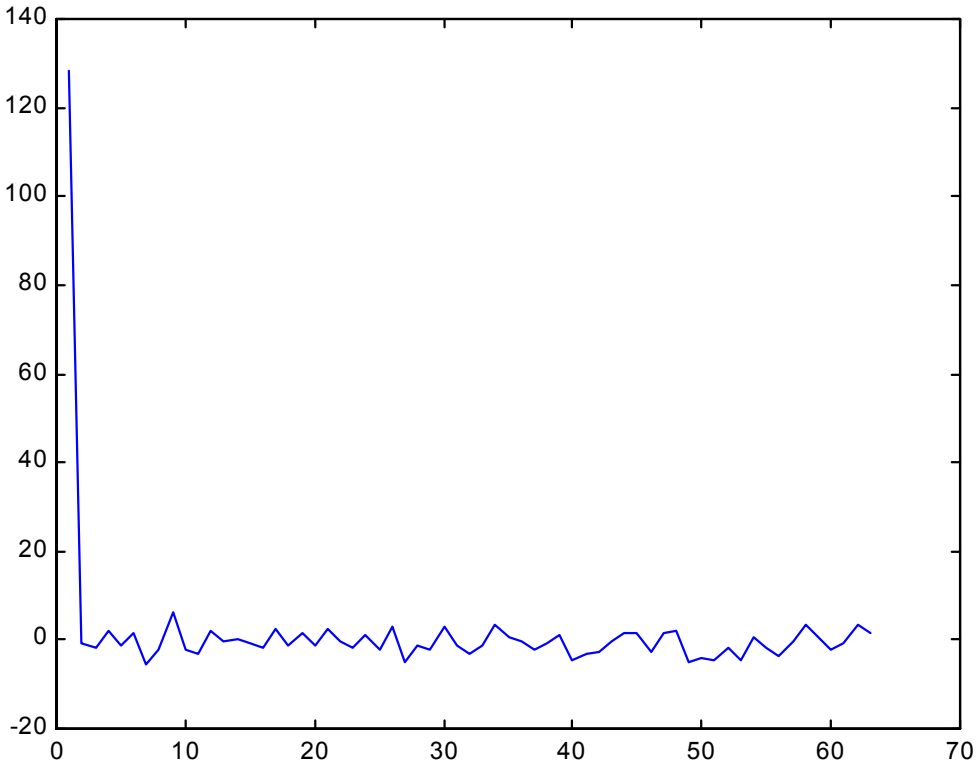

Figure 4-23. Code with taps at 7 1, noise added correlated with reference code with taps at 7 1.

Chapter 5 - Experimental Effort

The proof of this system is, of course, with the experimental effort to see what results can be obtained when hardware and software are combined together and tested. In performing the experimentation, the two distinct sensors were placed in the optical fiber communications system in such a way that they had their respective signals sent to the same fiber. The codes were generated using standard flip flop registers and the signals received at the detector were analyzed with the software specifically designed to receive the different sensor signals.

5.1 Experimental Setup

As mentioned in Chapter 4, the experimental setup is shown diagrammatically in Figure 4-1. The two different sensors have code generators associated with them and these send pseudorandom pulses to the LED's which then emit light at 820nm into the 62.5/125 multimode graded index optical fiber. The light from the fiber optic sensor LED goes through a coupler and then into the intensity-based sensors. The modulated light from the sensors is then combined through another coupler so that information from both sensors is now on one fiber. Note the delay coil in one arm of the fiber optic sensor setup. This is to delay the transmitted light approximately one pulse time so the detector can discern one fiber optic sensor signal from the other.

The light from the MEMS code generator is modulated by the MEMS sensor as shown in the figure. The modulated light from this sensor is combined with the light from the fiber optic sensors and is then coupled into the receiving fiber via an optical coupler. The combined light pulses are then sent optically to the detector where they are converted into analog electrical information, read by the oscilloscope, and to the computer for signal processing.

Figure 5-1 is a diagrammatic representation of the two code generators. Two 4 bit shift registers are connected together to provide a shift register capable of operating at 2 through 8 shift sequences. For ease of experimentation, both registers were connected using 7 stages total per generator. Taps 1 and 7 were used for the fiber optic sensor generator, and taps 3 and 7 for the MEMS sensor generator. This resulted in codes that have a relatively low cross correlation of 17. This was necessary so the software could separate or demultiplex the two different signals.

5.1.1 Design of the Code Generators

The schematic of code generators is shown in Figure 5-2. The generators for both the fiber optic and MEMS sensors are identical except for the taps which control the type of code generated. The MEMS sensor also has a modulation circuit to vary the intensity of its LED.

The pulsed output of the clock is inputted into the clock connections of both of the four stage shift registers. The output of the first shift register, pin 12, is connected into the first stage of the second four-stage shift register. The output of this shift register (here stage 3 which, when added to the first shift register, gives 7 total stages) is fed into the adder. In the case of the fiber optic sensor, stage 3 of the first shift register is also fed into the adder. In the case of the MEMS generator, the output of stage 1 is also fed into the adder. The output of the adder is then fed into the input of the first shift register. The maximal bit length sequences are then taken from the stage 7 output (pin 13 on the second register) and fed into the LED drivers. In both cases, the drivers are set up so that the LED input is shorted out by transistor Q1 as the pulses are generated. In the case of the MEMS sensor, the LED output is modulated by transistor Q2 connected to the MEMS sensor.

5.1.2 MEMS Sensor Modulation and Code Generation

Code generation and modulation of the MEMS sensor is accomplished by the circuit shown in Figure 5-3. Here the code is generated by a circuit identical to the fiber optic sensor code generator, but the LED is triggered by an additional NPN transistor. The LED is shorted out with each pulse and the amplitude is controlled by the ADXL-05 sensor providing voltage to the base of the transistor. As the voltage changes, the amplitude of the light from the LED is varied as a function of input voltage which is controlled by the transistor. This modulation scheme was chosen in favor of a simple on off switch since the operational frequency uppper limit of the ADXL-05 is Hz and the LED is switched on and off at a rate of 1.8 MHz.

The overall experimental setup is shown pictorially in Figure 5-4. On the left is the spool of fiber containing the fiber optic sensor delay coil. To the right of the delay coil is the fiber optic sensor and coupler assembly consisting of three couplers and two intensity-based fiber optic sensors. To the right of that are the code generators constructed on the breadboard assembly. The MEMS generator is on the left and the fiber optic sensor generator is on the right. The MEMS Sensor Assembly is in the foreground. Next to the breadboard assembly is the LeCroy oscilloscope which is connected to the Hewlett Packard detector. The oscilloscope reads the voltage across the detector which is proportional to the incoming optical signal. A view of the fiber optic sensor assembly, code generators and MEMS sensor assembly is shown in Figure 5-5.

5.2 Experimentation

The steps in the experimentation were as follows: As part of the overall signal processing, the reference codes from each code generator were sent separately into the detector and stored as a file on the computer. These codes were normalized and then converted to RMS, and then the autocorrelation of each of these resultant normalized RMS codes was taken to ensure that a valid

MLBS was indeed sent out and then stored. The returned signal was correlated with each of the sent codes to determine the sensor values.

5.2.1 Results

The system succeeded in multiplexing the two different signal sources and then separating them out with the software. The results are shown in Figures 5-6 through 5-19. Figure 5-6 , and the corresponding return, Figure 5-7 show the theoretical output of the initial pulse that is used to interrogate the fiber optic sensors and the corresponding theoretical return. Figure 5-8 shows the theoretical correlation of the two pulses. Figures 5-9 and 5-10 show experimental pulses sent out and then received at the detector. The and 5-9 show the actual pulses that are sent out and the raw return data is shown in Figure 5-10. It is this raw return data that is fed into the software-based signal processor.

The results of the cross correlation is shown in Figures 5-11. There are two peaks, each representing one fiber optic sensor. Note how this output compares with the raw return data. The raw return data appears virtually unintelligible to the naked eye, however, the correlated data contains the two well defined peaks. This is to be expect and closely parallels the expected theoretical output.

5.2.2 MEMS Sensor Results

A key to success was to discern the MEMS sensor with the system, in view of the fact that the main goal was mulitplexing different sensor signal sources using software and signal processing. The results of the MEMS sensor running through the code division multiplexer are shown in Figures 5-12 through 5-14. Figure 5-12 is the outgoing MEMS sensor pulse and Figure 5-13 is the received pulse. Figure 5-14 is the cross correlation of the received pulse with the outgoing pulse. Note the poeak at approximately t=170. This represents the output of the MEMS sensor..

Note that it is quite similar, as one would expect, to the triangular peaks of the two fiber optic sensors shown before.

Figure 5-15 shows the same raw return data where the correlation is now taken to discern the two fiber optic sensors. Notice that again there are two peaks, each representing a fiber optic sensor. It is also important to have no peak when there is no signal. Figure 5-16 shows what happens when the MEMS sensor signal is zero and the received signal is correlated with the MEMS sensor outgoing code. There is no discernible correlation. The same is true for Figure 5-17 when the fiber optic sensor is zero.

5.2.3 Timing

The signal processing system was modified and the experiments described above were repeated using a non-synchronized set of codes. A separate 1.8432 Mhz crystal was installed to drive the fiber optic sensor code generator. Key results are shown in Figures 5-18 and 5-19. Here, again, the MEMS and fiber optic sensors are readily discernible when correlated with their respective codes. It should be pointed out here that the synchronized code generators were synchronized in terms of pulse times only. That is to say that both the MEMS and fiber optic sensor codes differed by exact multiples of pulse times. With the non-synchronized approach, the difference was of a continuous variety. The issue of timing is important since the use of the system to multiplex a large number of different type sensors would not allow for synchronization of each code generator.

5.3. Summary of Experimental Results

The overall goal of discerning the two different types sensors, MEMS and fiber optic was acheived through the use of signal processing software specifically written for this research.

Unprocessed received signals are so weak before being processed that they cannot be discerned by the naked eye.

After the signal processing performs the autocorrelation, the signal can be read and converted to an actual sensing value.

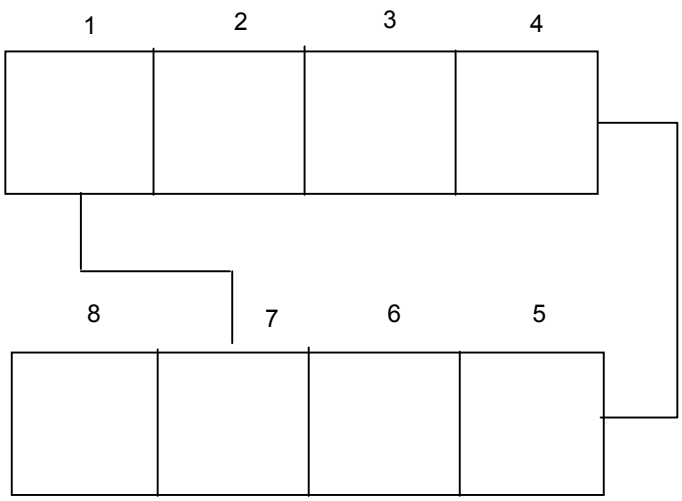

Figure 5-1. Diagrammatic Representation of Shift Register. Taps 1 and 7 Connected.

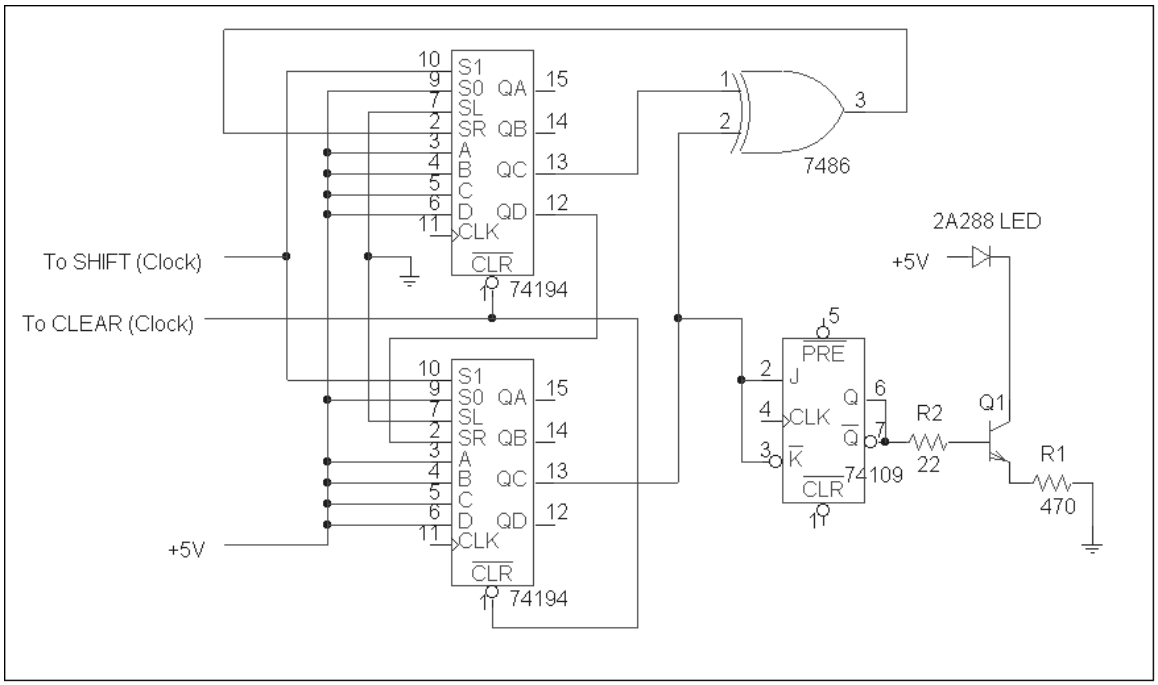

Figure 5-2. Code Generator Schematic for Fiber Optic Sensors.

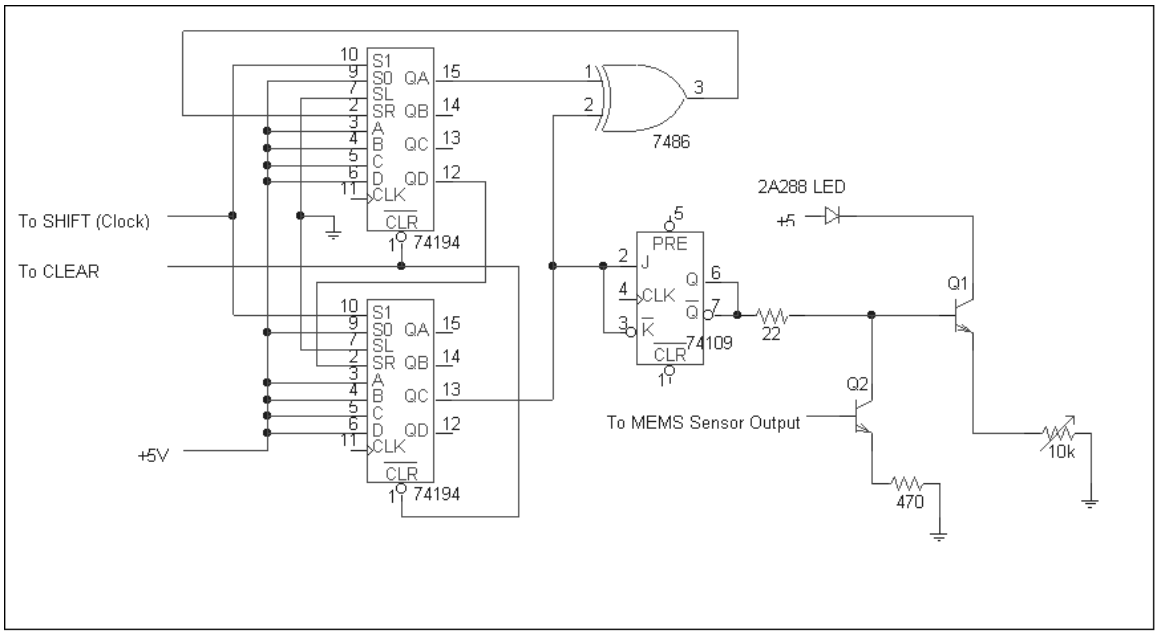

Figure 5-3. Code Generator Schematic for MEMS Sensor.

Figure 5-4. Overall Experimental Setup.

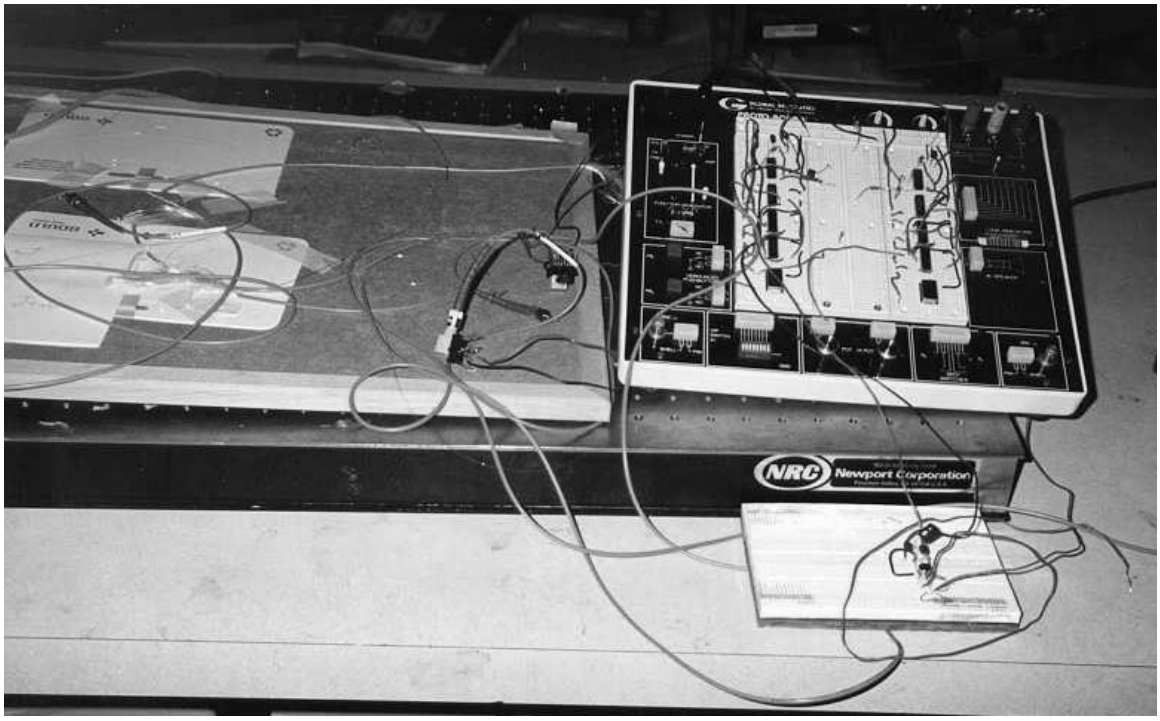

Figure 5-5. Experimental Setup; Fiber Optic Sensors (left), Code Generators (right), and MEMS Sensor (foreground).

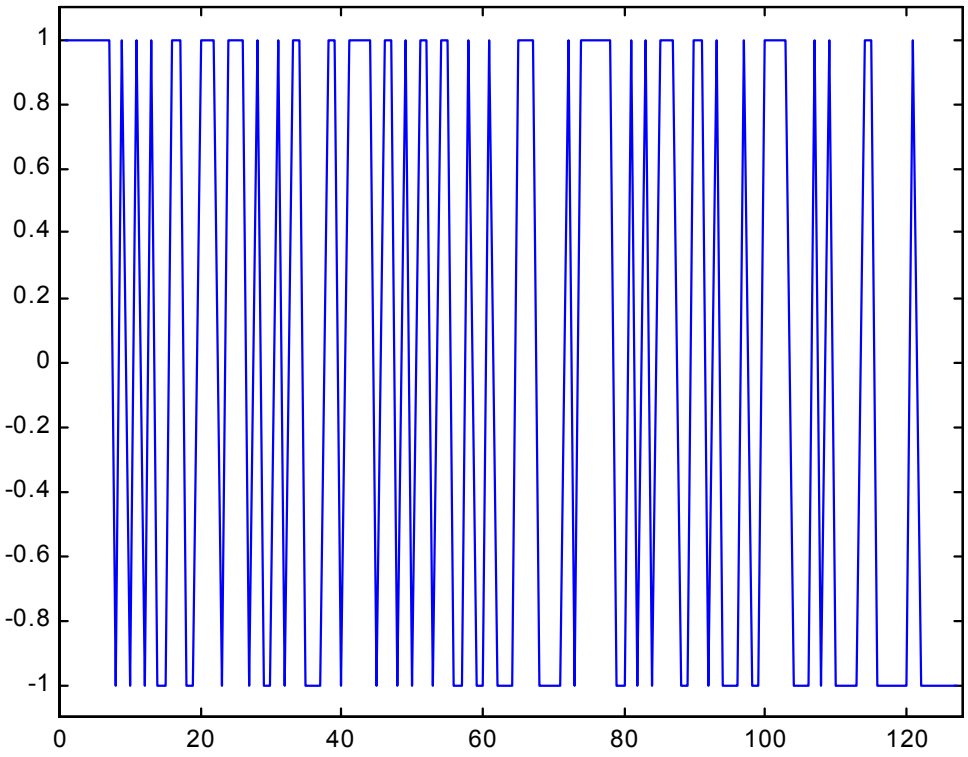

Figure 5-6. Theoretical Pulse Output.

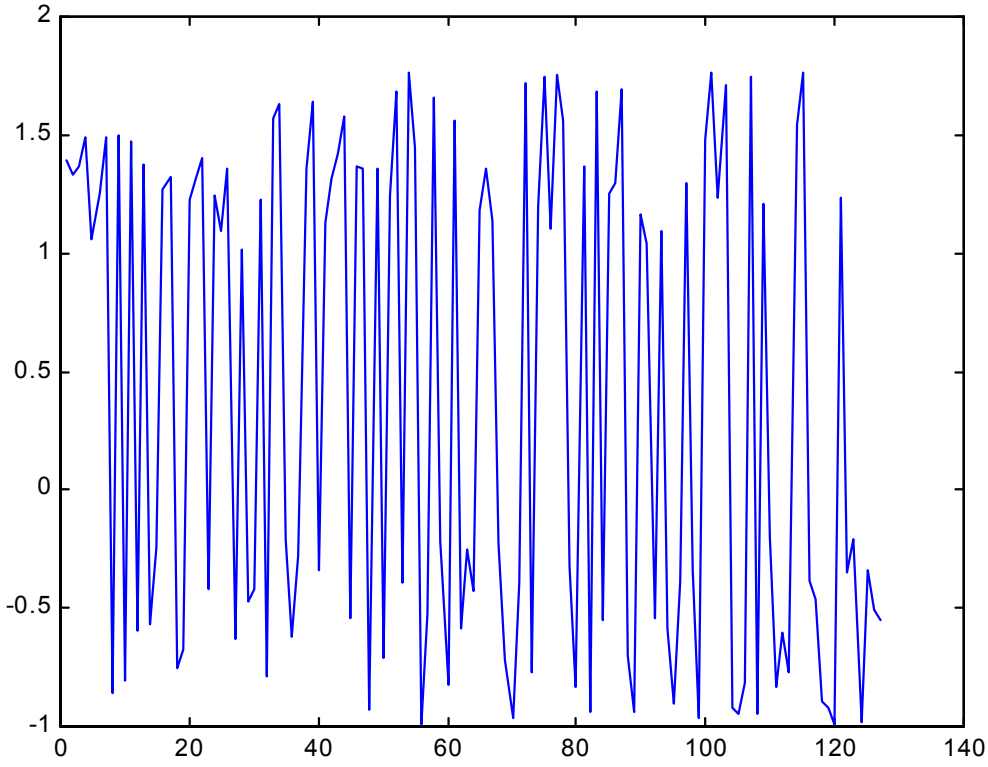

Figure 5-7. Corresponding Theoretical Return (Noise Simulated).

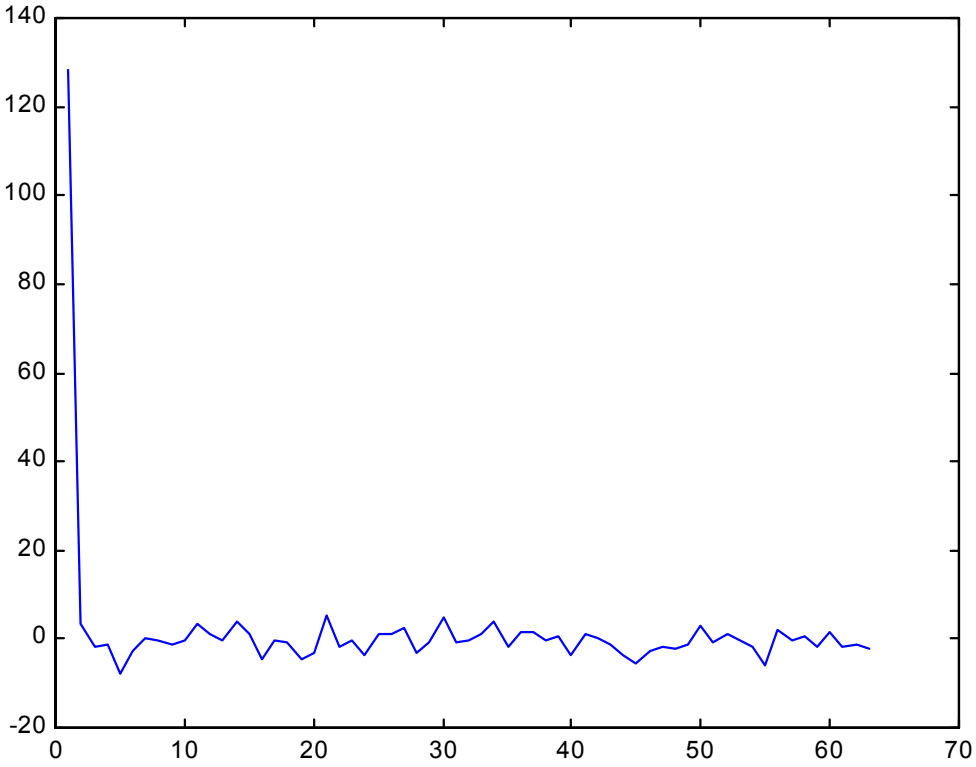

Figure 5-8. Corresponding Theoretical Peak for FO sensors.

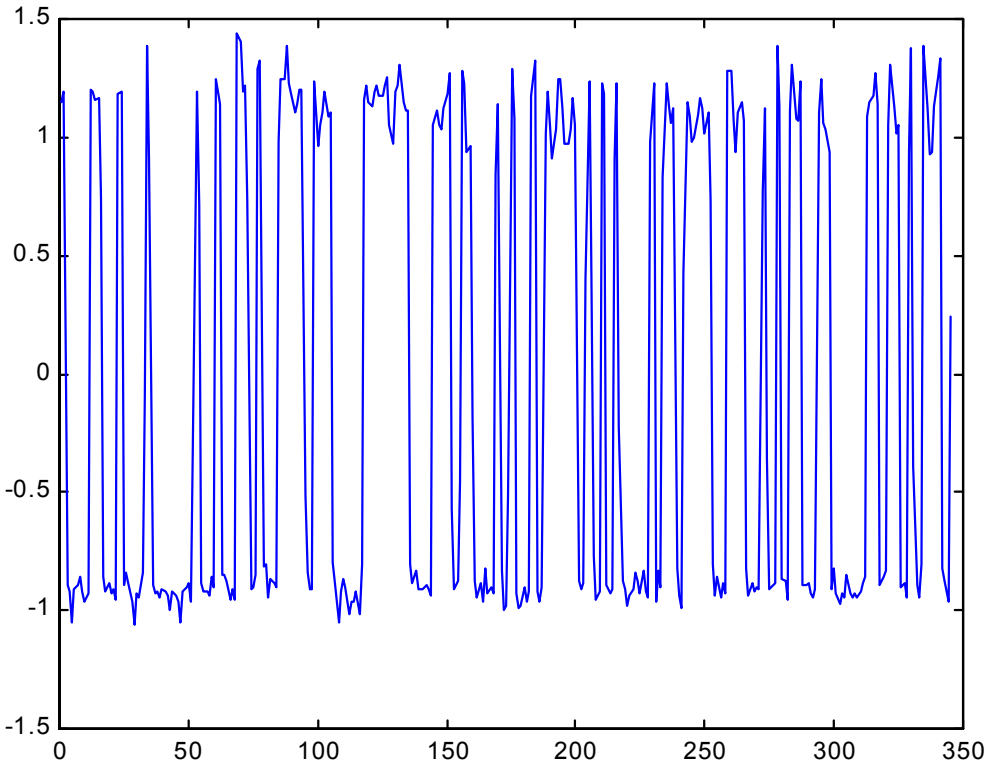

Figure 5-9. Experimental Fiber Optic Sensor transmitted pulse.

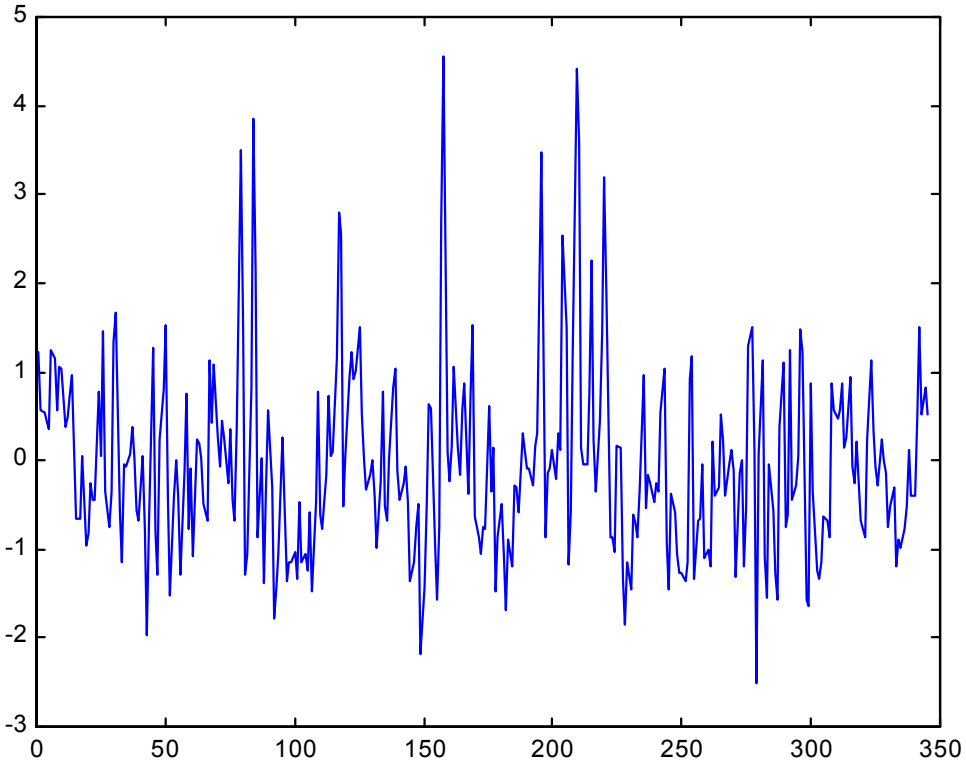

Figure 5-10. Experimental Fiber Optic Sensor Return.

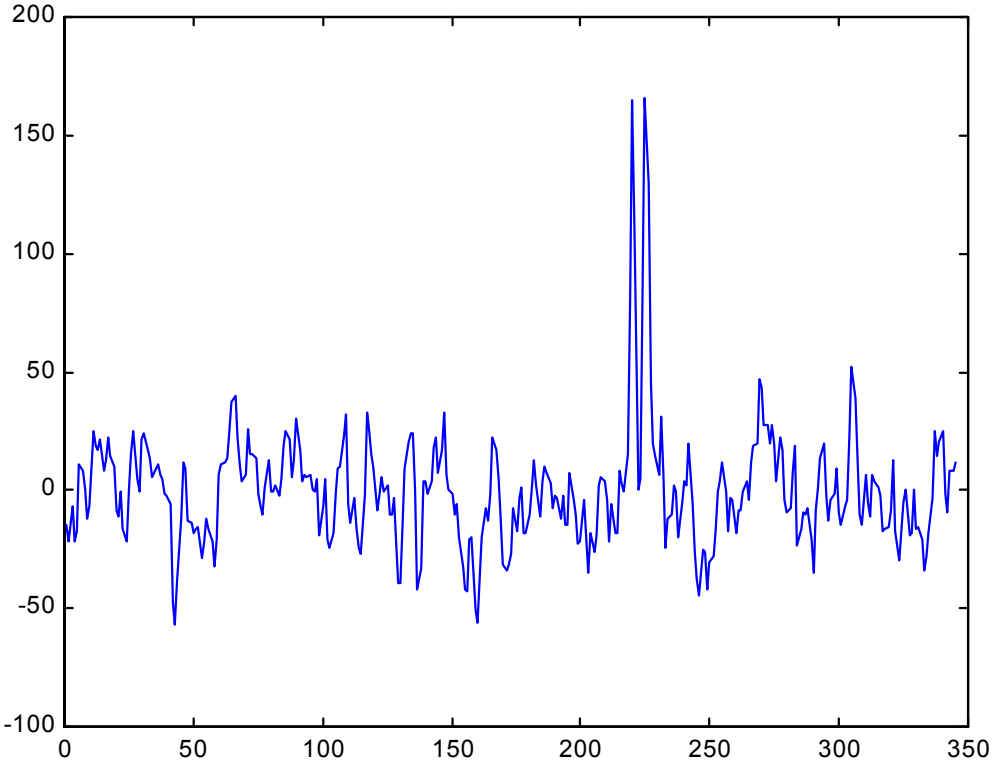

Figure 5-11. Corresponding correlations (FO sensors only).

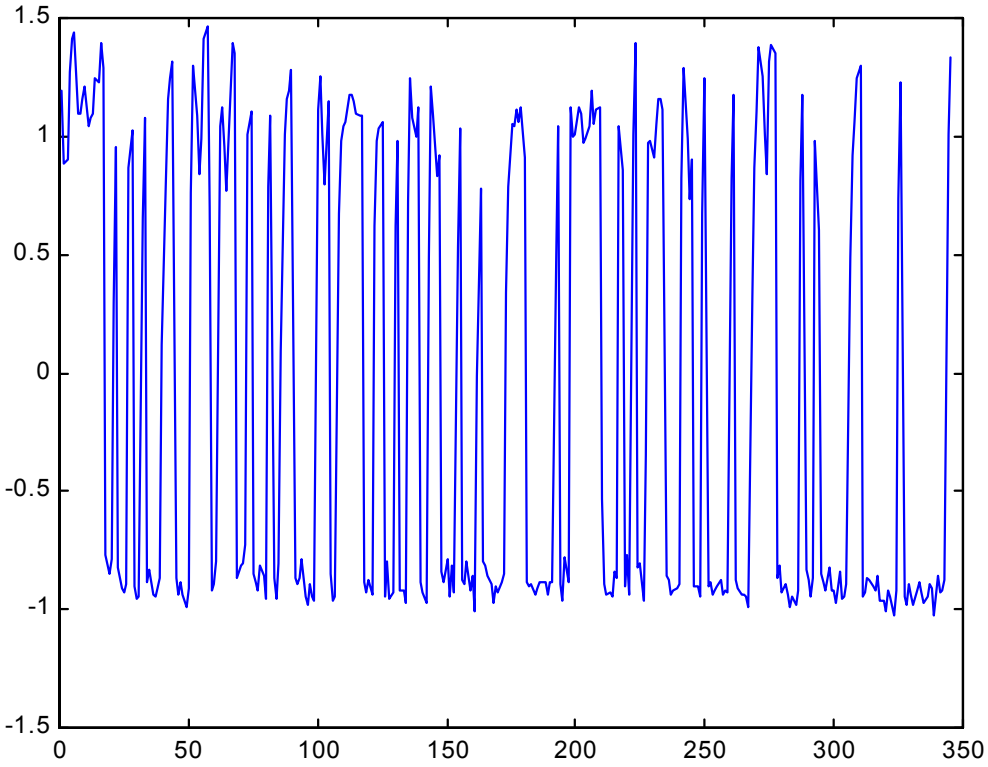

Figure 5-12. MEMS outgoing pulse.

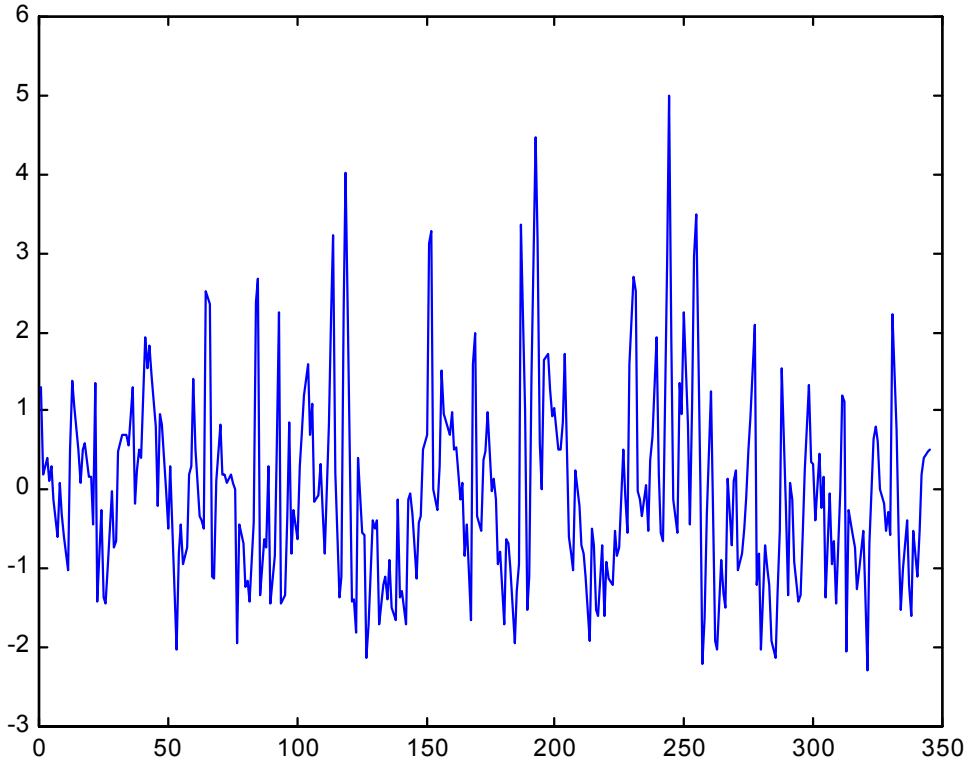

Figure 5-13. Experimental MEMS return pulse.

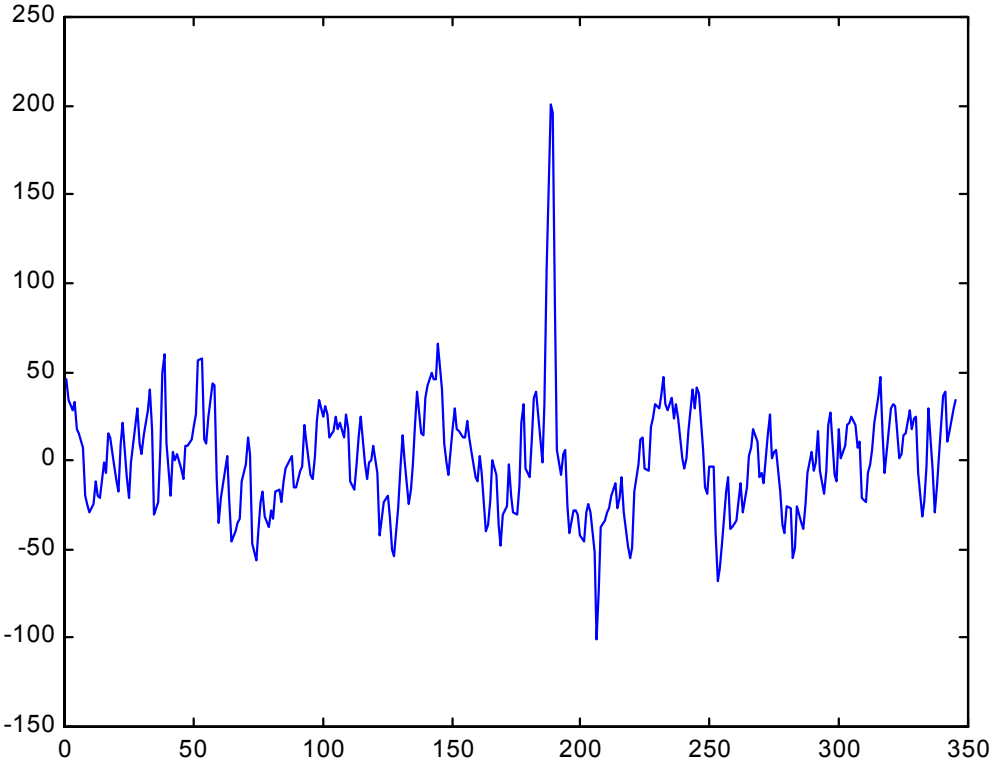

Figure 5-14. Correlation of MEMS pulse. Note the peak at t=170.

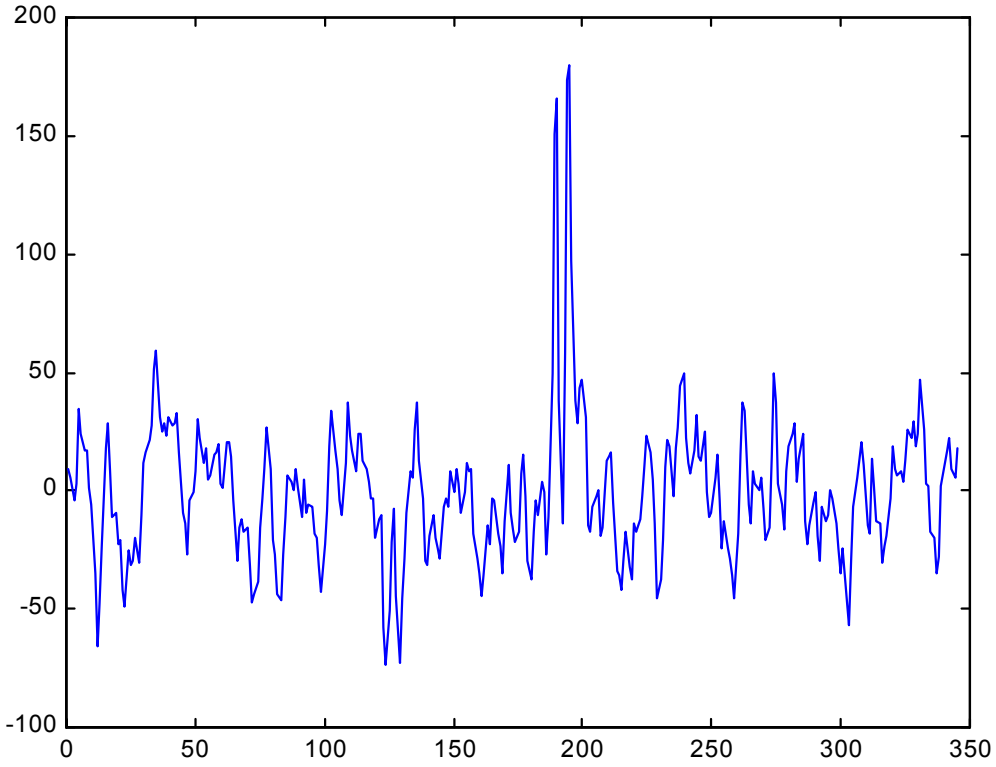

Figure 5-15. Same returned pulse, but correlated to detect FO sensors.

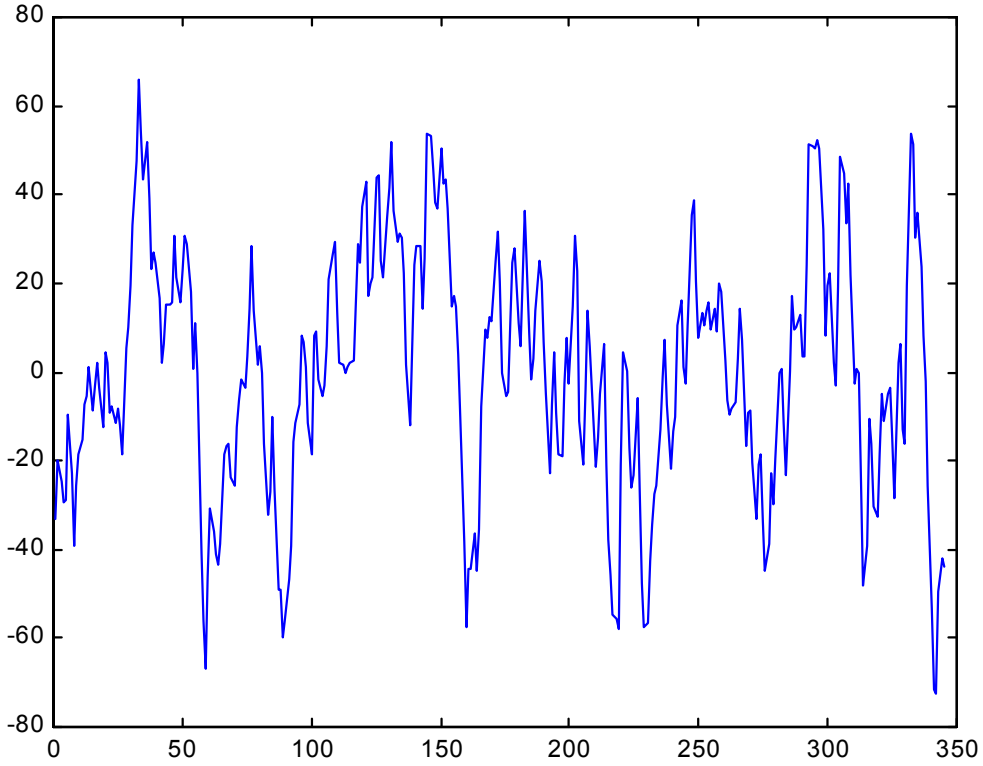

Figure 5-16. Correlation of MEMS sensor with zero MEMS signal. Note lack of correlation.

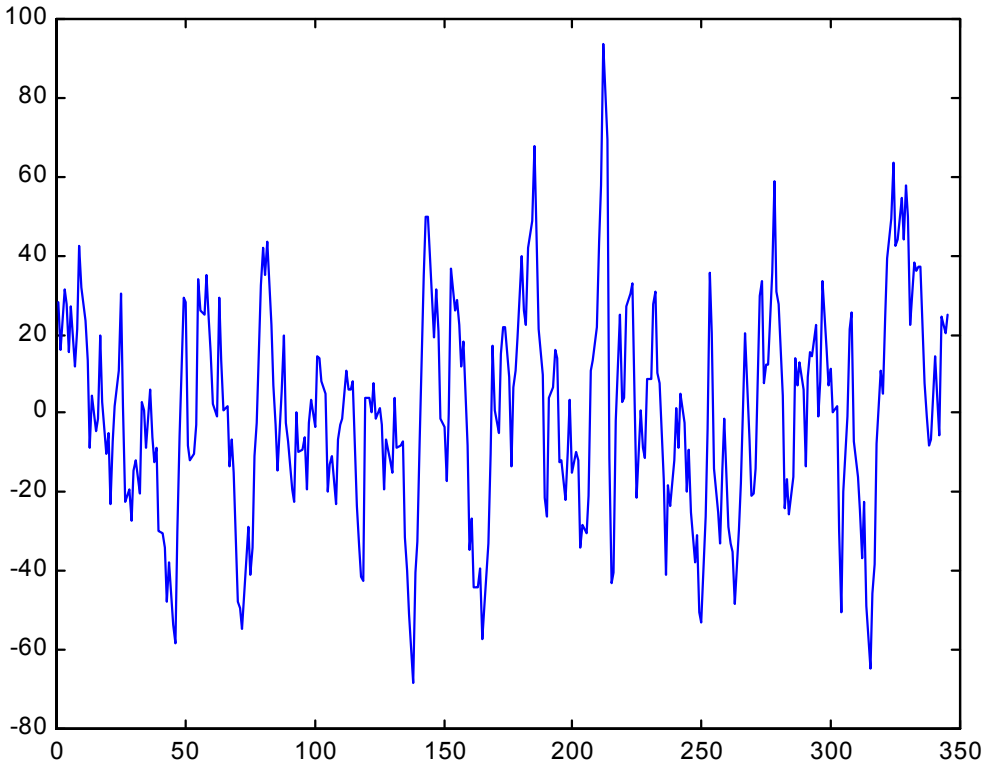

Figure 5-17. Correlation of Fiber Optic Sensors with zero signal Note lack of correlation.

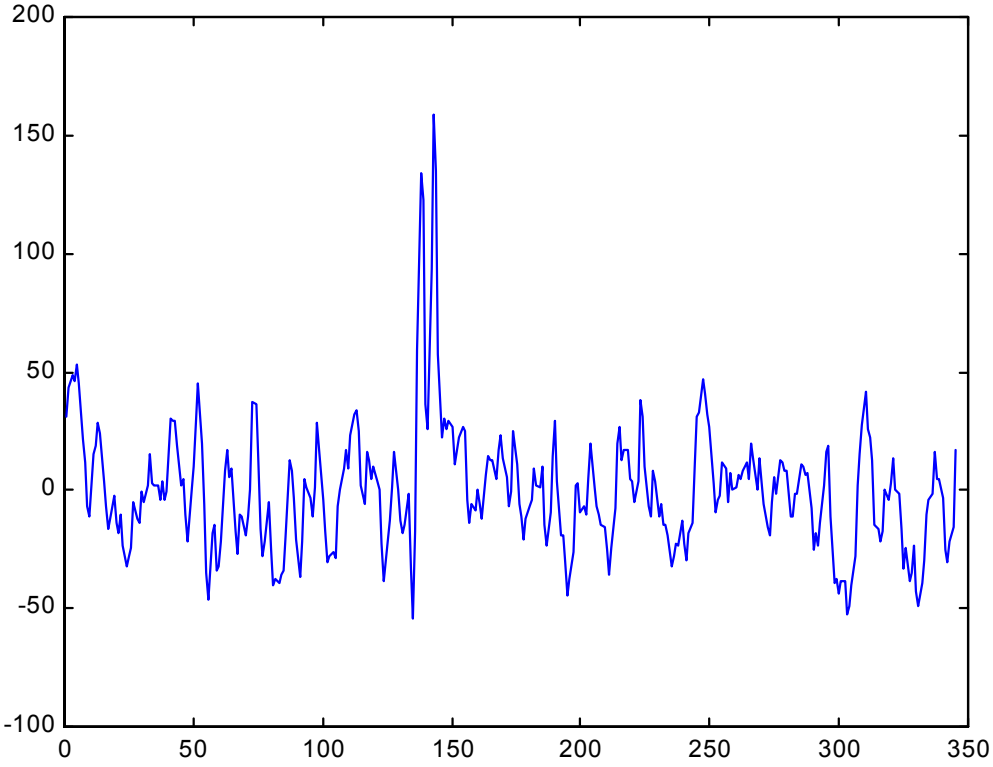

Figure 5-18. Unsynchronized generators; Fiber Optic Sensors.

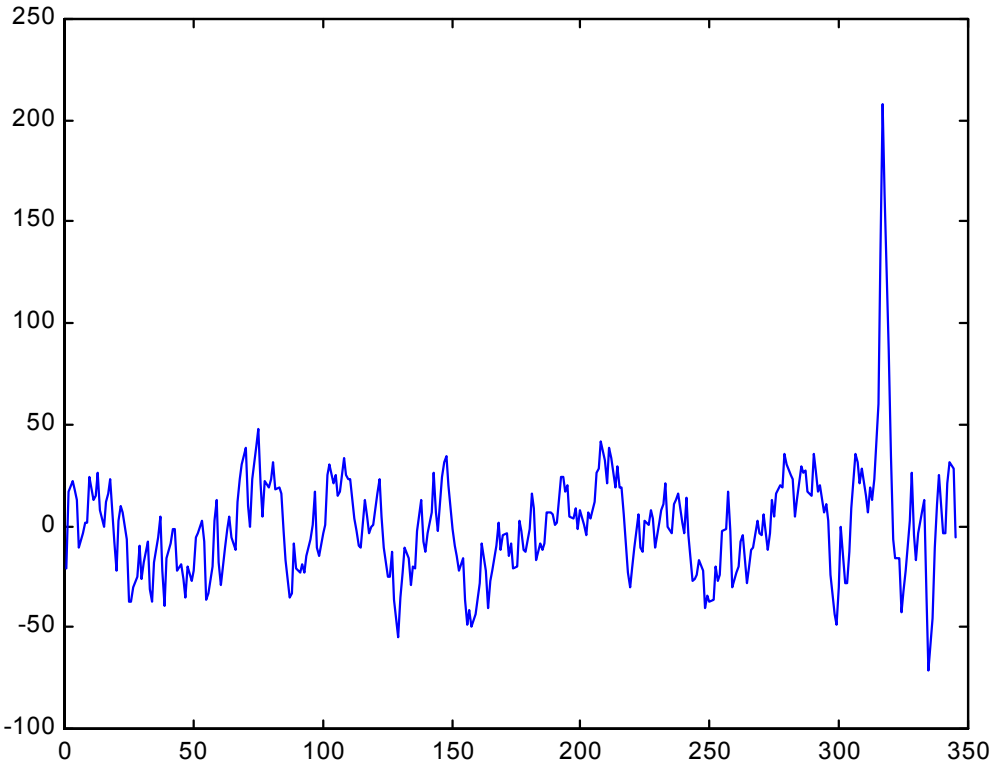

Figure 5-19. Unsynchronized generators; MEMS Sensor.

Chapter 6 - Analysis of System Limitations

When considering a system of the sort described in this dissertation, one must consider the results when the system is expanded. The primary limit is the number of sensors, and if the system is expanded beyond what was demonstrated, i.e. the two fiber optic and one MEMS sensors, other limitations come into play. Recall that the desire is to have a large system of mixed signal sensors. These limitations include bit error rate limitation on sensor resolution, time jitter, number of codes, physical device limitation, response time, and system topology.

6.1. Limit on the Number of Sensors

There are two limits to consider when looking at the upper bounds of the number of sensors: fiber optic sensor limits and MEMS sensor limits. With the fiber optic sensors, half the power is lost as the number of sensors doubles. This can be expressed by,

$$P = \frac{P_T}{P_R} = N,$$

where P is the ratio of optical output power P_T and the received optical power, P_R, and N is the number of fiber optic sensors connected in a tree network. As the number of sensors is doubled, twice as much optical power is required for a given code length.

As the code length is increased, the number of sensors can be increased. The correlation is similar to that of the power increase and is given by

$$P = \frac{P_T}{P_R} = CL,$$

where CL is the code length and is given by

$$CL = 2^{BL} - 1,$$

where BL is the bit length of the shift register. For most code lengths we can ignore the -1 and, combining equations, we obtain

$$N = 2^{BL}.$$

This again means that as the code length doubles, the maximum number of sensors doubles, or, as the bit length of the shift register increases by one, the maximum number of sensors doubles.

A graphical representation of this is shown in Figures 6-1 through 6-4. We can see that when increasing the power 8 times over what is required for one sensor, we can have a maximum of 250 fiber optic sensors. But when we go from 8 to 12 times over the original power level, we can get 4000 sensors. Similar increases are true when the code register length is increased, as shown in Figures 6-2 and 6-4. However, notice what happens when both the code length and the optical power are increased by a factor of 12 as shown in Figure 6-5. The total maximum number of sensors is over 8 million.

The limit on the number of MEMS sensors is a different story. The limit is not governed by power since each MEMS sensor has its own optical transmitter. Also, each sensor adds to the noise when the detector is attempting to discern a particular sensor. So as long as there is adequate power to overcome a few couplers, the number of MEMS sensors can be increased without respect to power. What is an issue, though, is the number of allowable codes. For a

given code length, there is a finite number of codes that can be used to transmit information. The number of allowable codes versus code length is plotted in Figures 6-6 and 6-7 below.

6.2. Bit Error Rate Limitation on Sensor Resolution

This system is a combination of digital and analog components, i.e. while the overall sensor signal measured is indeed analogue, a digital code is also used. If some bits are transmitted in error, it will affect the code received and will also affect the analog signal that is received. It may well mean that no signal is received at all.

An accepted figure for bit error rate of a system is $10^{-9,}$ which means one bit is transmitted in error for every 10^9 bits transmitted. If codes can be kept to a maximum length of 10^9, the system will perform satisfactorily. This is a new limitation on the code length since earlier it was shown that it was desired to make codes as long as possible. The tradeoff is a maximum code length of 10^9 which corresponds to a register length of 33. Looking again at the figures of the three dimensional plot, we see that this is not a problem since the maximum length required would be a register of length 12. If bit error rate did become a problem, i.e. we did decide to use extremely long codes, error correction could be used. Another scheme would be to modify the system so that the codes were continuously transmitted and an average taken.

6.3. Physical Device Limitations

This research used intensity-based fiber optic sensors, but other devices could also be used. One of these is the Fabry Perot sensor which has a reflectivity of 1-10 percent depending on the particular sensor, and would therefore require longer codes or more power. If Fabry-Perot sensors are used, high reflectivity is desired. In short, any device that reduces power significantly should be avoided, but even these can be used if code length and/or power are increased.

As far as the MEMS sensors go, they could be used with few limitations. The MEMS sensors can have artificial intelligence at the sensor, but this is not a requirement. One issue that arises though, is that as the code length grows, the MEMS sensors will have to have more computing power at the sensor just to generate a longer code. This could mean a higher speed processor and resultant cooling problems. But, as computing power limits continue to increase, this should not be a major issue. Also, since the power output of the MEMS sensors does not have to increase, the LED portion of the sensor can remain relatively simple.

6.4. Time Jitter

Time jitter is a factor in that it can lead to the wrong code being received if the jitter is greater than one pulse time. It is important to note, though, that synchronization of the MEMS sensors is not necessary due to their inherently different codes.

A sample calculation shows the effect of jitter. If a 1.8 MHZ clock is used, each pulse length is 5.5×10^{-7} seconds or .55 microseconds. Since jitter is typically in the picosecond range, there would not be a problem until a frequency of 100 MHZ was reached.

6.5. Response Time Of The Sensor Network

As the system is expanded, the overall network response time could become an issue. Since sensors typically sample at low data rates (one measurement per second or less is not uncommon) and the system can be constructed with high speed communications devices, response time is not an issue as long as a receiver is fabricated that reads the signals continuously.

6.6. System Topology

Five basic topologies; bus, tree, ring, star and mesh were considered. The system in the experimentation used a tree topology, and other topologies could also be used but caution should be exercised. The ring and mesh topologies could lead to multiple signals being received due to a ghosting effect. If there is more than one path from the optical source to the receiver, ghosting will be a problem.

One solution to this would be for the receiver to expect the multiple signals and allow for them. This could be accomplished by sophisticated detection circuitry. The advantage of using a mesh or ring topology is that redundancy is built in. If there is a break in one of the fibers, the others could pick up the slack.

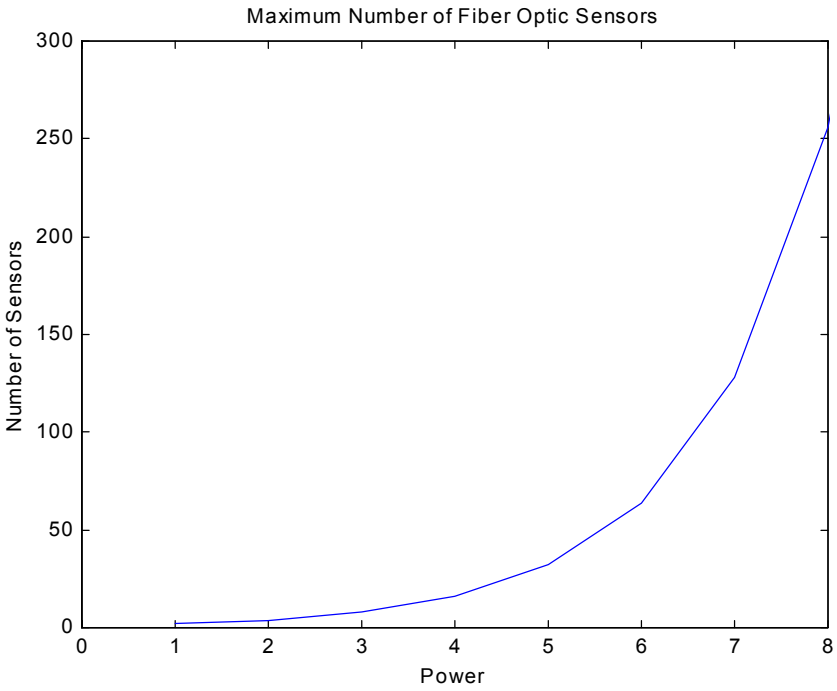

Figure 6-1. Maximum Number of Fiber Optic Sensors vs Power

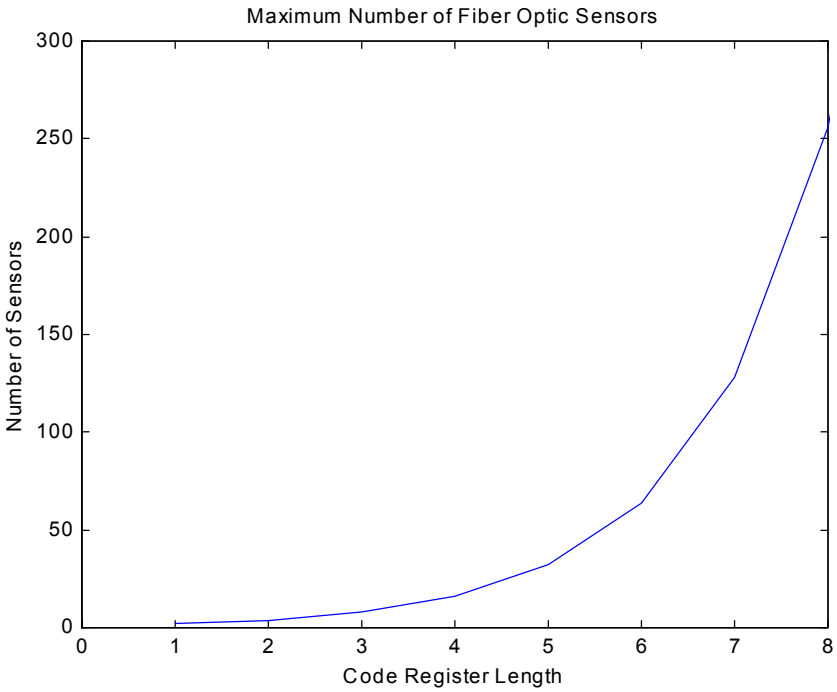

Figure 6-2. Maximum Number of Fiber Optic Sensors vs Code Register Length

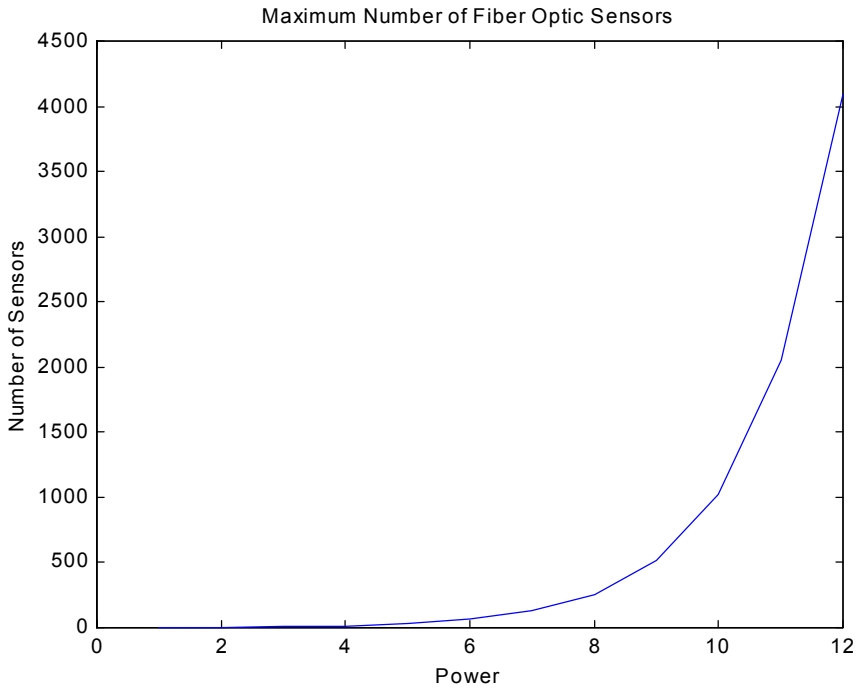

Figure 6-3. Maximum Number of Fiber Optic Sensors vs Power - Graph Extended

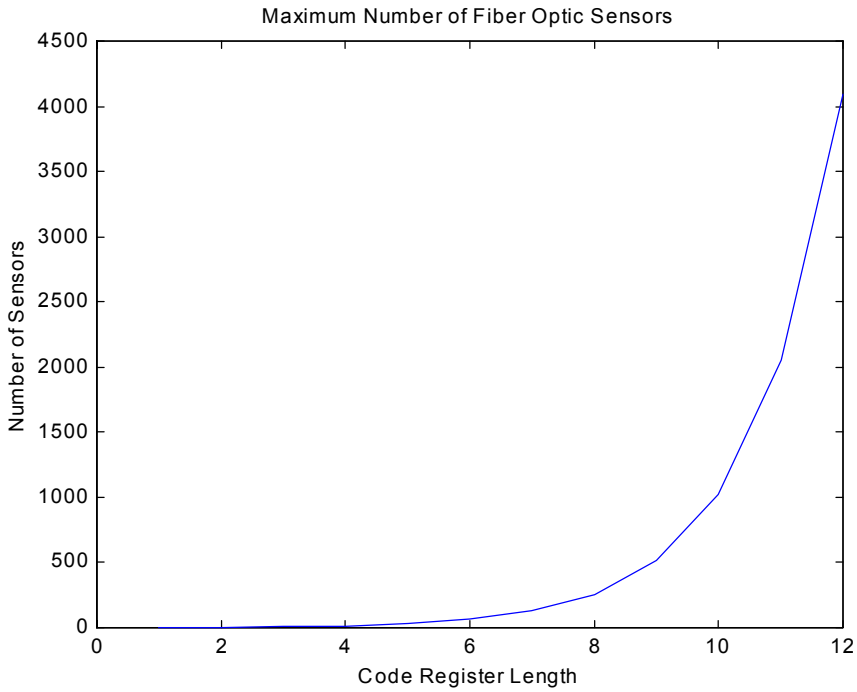

Figure 6-4. Maximum Number of Fiber Optic Sensors vs Code Register Length - Graph Extended

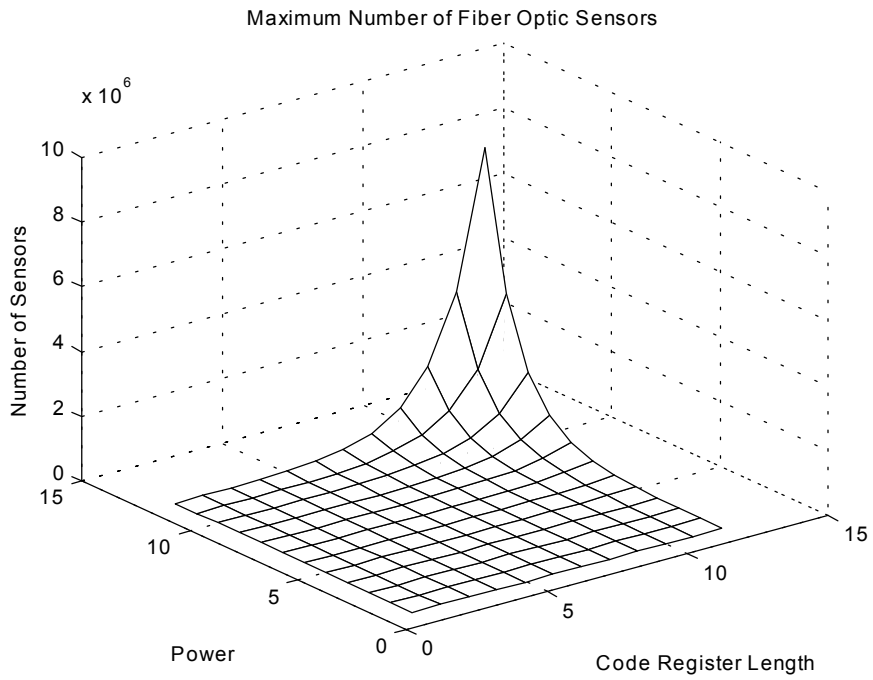

Figure 6-5. Maximum Number of Fiber Optic Sensors vs Power and Code Register Length

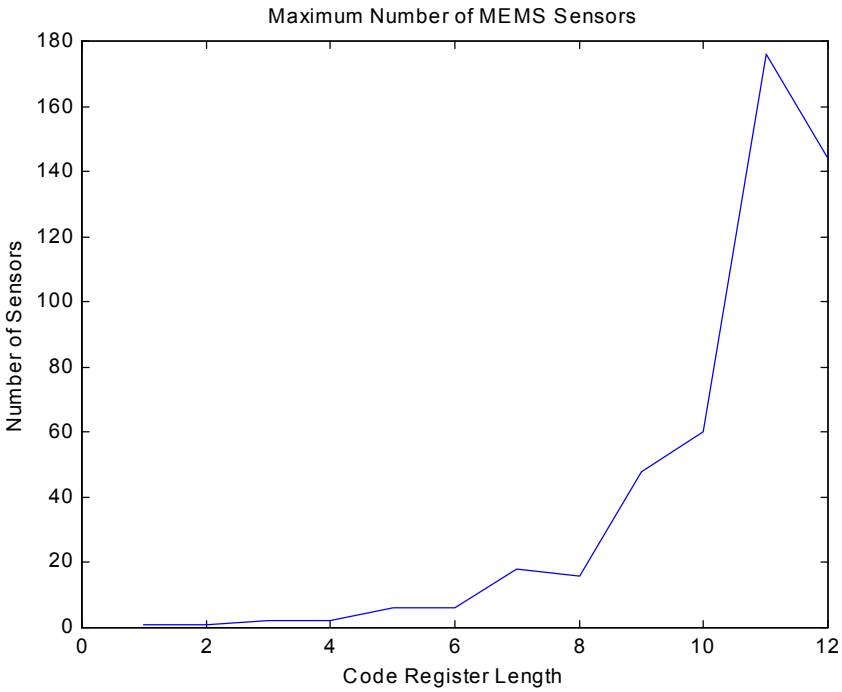

Figure 6-6. Maximum Number of MEMS Sensors vs Code Register Length - Power Constant

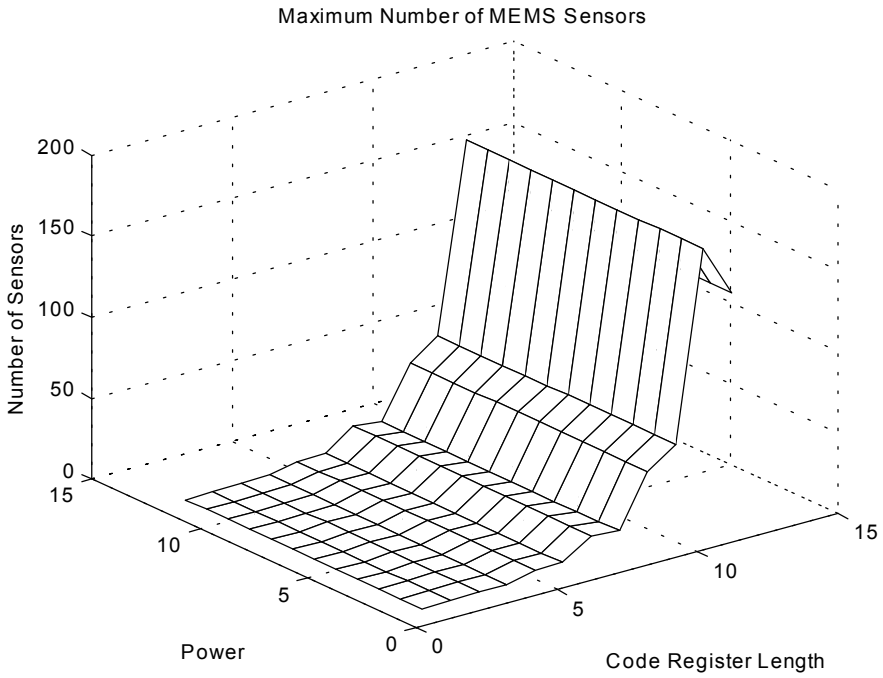

Figure 6-7. Maximum Number of MEMS Sensors vs Code Register Length - Power Constant. Three Dimensional Representation

Chapter 7 - Example - Naval Shipboard Multiplexed Networks

While this dissertation has demonstrated successfully the integration of MEMS and fiber optic sensors using software and signal processing techniques, it has only been a laboratory demonstration. The real test is in a network that connects large numbers of different-type sensors. While this type of test is beyond the scope of this dissertation, I address here the issues to be considered to allow the system to be used on board a Navy ship.

The United States Department of the Navy has been directed to acquire ships that have a very low level of manning.[7.1, 7.2] The are several events which must take place for this to be accomplished. One is the installation of a large number of shipboard sensors, all of which must be networked together. Some estimates indicate that as many as 250,000 sensors will be installed on a single ship compared to the current number of 2300. [7.3]

These future shipboard sensor networks will consist of several kinds of sensors: Discrete (on/off), continuous reading, fiber optic, MEMS, wireless and conventional electromagnetic. While the exact design has not yet been determined, one thing is for certain: Fiber optic and MEMS sensors will most likely play an important role.[7.3] This is because fiber optic sensors are immune to electromagnetic interference (EMI), and MEMS sensors have the advantage of being small and inexpensive when manufactured in large quantities.

The purpose of the reduced manning effort and therefore the large number of sensors is the serious budget problems the Navy is facing. Therefore any effort that enables reduced manning must in itself be cost effective. Not only do the sensors have to be as inexpensive as possible, but the networking must have a low cost as well. While it might be desirable to have each sensor connected to a node on a network, it is easy to see that this would be cost prohibitive since a quarter of a million nodes would be needed. What is needed is a cost effective way to meet the sensing and networking needs for the future Navy ships.

The environment on board a Navy ship is very harsh for sensitive electronic and optical equipment. Temperatures can reach one 100 degrees Fahrenheit and humidity can be as high as 95 percent. Another environmental concern is one of shock due to nearby explosions. The issue of shock is a common one on Navy ships and it is usually dealt with by mounting sensitive equipment in shock resistant cabinets.

Another consideration for use of this system onboard Navy ships is the manufacturing ability of the sensors and system. This dissertation demonstrated that commercially available equipment can be used in the code division multiplexing system. One advantage of the system is that the complexities are transferred from the optics to the computer and software. This is not just an aesthetic decision. It allows one to take advantage of the cheap computing power that is now available due to the high volume of personal computer sales.

Other considerations that must be taken into account include: relatively dirty environment, accuracy of measurement, and compatibility with other equipment. The relatively dirty environment can be a problem for any type of equipment, and is especially true with optical equipment. However packaging techniques now available can make many types of components immune to the dirty environment.

Most of the sensors to be used on the ships of the future do not have to have a high degree of accuracy. Typical applications would include major the machinery temperature measurements, and plus or minus one degree Fahrenheit would be adequate. Pressure measurement in various piping and fluid systems is another application and plus or minus one percent would be adequate with only a small number of sensors requiring extreme accuracy. Therefore it is much better to use simple low cost sensors that can be manufactured cheaply for the system. As mentioned earlier, using artificial intelligence on the MEMS sensors could predict catastrophic conditions or maintenance actions. While accuracy would not need to be high, transferring the computing power to the MEMS sensor would be necessary.

Compatibility with other equipment and networks is a major naval shipboard consideration. While I have described this system for the purposes of this dissertation to be a network, in Navy terms it is really a "sub-network ". This means that the system must be able to connect seamlessly into the main communications networks. A typical schematic of such a system is a shown in Figure 7-1 [7.3]. A look at this diagram shows why a sub-network of sensors is necessary as opposed to one sensor per node connected to the fiber optic backbone. The cost of the nodes alone given a large number of sensors would be prohibitive.

Other Naval shipboard considerations include housing all the equipment so that it is tamper proof. When a ship is at sea, repair of equipment becomes paramount. If a complex sensor system is not secured, it can be tampered with by the sailors. One can easily see that catastrophe could be sure at hand. All of software and computers would have to be locked up and be made safe from unauthorized personnel. Additionally, training in the operation of the equipment would have to be made available to the sailors so they could perform routine maintenance and repair.

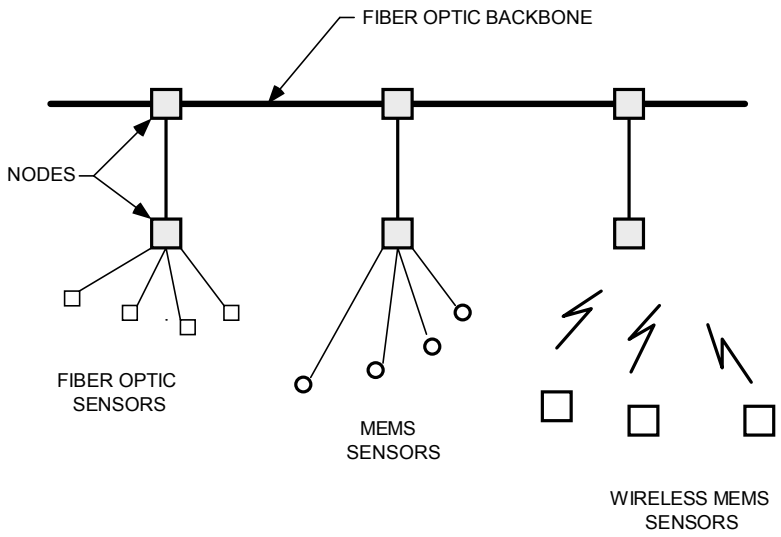

Figure 7-1 [7.2]. Proposed Future Naval Shipboard Sensing Network.

Chapter 8 – Conclusions

This dissertation has explored the idea of combining signals from totally different devices, realizing that this area of research is just as fundamental as multiplexing communications signals. The technical barriers in this dissertation research are similar to multiplexed communications systems with the primary limit being the number of sensors one can multiplex on a network. That limit affects a number of interrelated parameters such as network topology, physical device limitations, code size, code configuration, increased complexity of the sensor devices, bit error rate limitations on sensor resolution and response time of the sensor network.

Networking a combination of fiber optic and MEMS sensors using code division multiplexing requires tradeoffs be made in the system design. The upper limit on the number of fiber optic sensors is primarily governed both by power to the optical transmitter and by the code length. Increasing one of these parameters can increase the maximum number dramatically, and increasing both power and code length by several orders of magnitude gives an upper limit of approximately eight million sensors. The maximum number MEMS sensors in the network, on the other hand, depends solely on the code length, since each MEMS sensor has its own optical transmitter.

While it is desirable to have long codes to increase the maximum allowable number of sensors, there is an upper bound to code length that is dictated by bit error rate limitations on sensor resolution. As long as the code length is less that 109, the bit error rate issue is not significant and the system will perform satisfactorily.

The physical device limitations on the sensors include an adequate amount of fiber optic sensor reflectivity to keep code lengths and power at a reasonable level. The MEMS sensors have little physical device limitations when used on this system, but increased computing power on the sensor could lead to some cooling issues. Time jitter is not an issue below 100 MHz and system response time is adequate since we are using high-speed communications designs on low speed

systems. System topology was a tree network, but other topologies could be used. Topologies which are multipath in nature would have ghosting issues to overcome, but these same topologies have an inherent redundancy that can allow for fiber breakage by rerouting signals through undamaged fiber.

Further development of this research could indeed lead to technological advances that parallel those we have seen in the communications industry. One prediction is thousands of mixed-signal sensors in an enclosed area multiplexed together as described in the research with one notable exception: No fiber. The transmissions would be made via optical transmitters and receivers, but the overall gain one gets by increasing both the power and the code lengths could over come the effect of no fiber. The received optical signal would be that which has been reflected off the walls of the space. This would make the system useful in areas where high electromagnetic interference is an issue, but wireless sensor interconnection is desired.

Another prediction is that the codes could become so long due to increased computing power that this system could be used to multiplex high speed computers with the "wireless optical" effect noted above. Since this research involves pulling signals out of the noise, one could envision portable communications devices that communicate long distances optically. All that would be needed would be for the light, after many lossy reflections, to end up at the receiver. Perhaps one of the biggest implementations of this technology in next-next generation systems would be devices that communicate optically over a long distance, say continents away. Once could envision a sensor planted at a strategic location say, in Asia, and being monitored in Washington DC, all through the code division process. One can also envision passive and active sensors being multiplexed, again wirelessly, to a central receiving point. Artificial intelligence on some of the sensors would process data, say earthquake vibration data, and send it optically through high EMI fields along with passive the sensor data to the central receiving point.

References

[1.1] "The Big Squeeze"available from http://bama.ua.edu/~trieland/tcf355/connections/tsld018.htm. INTERNET. Accessed March 16, 2000.

[1.2] "History of Internetworking," available from http://www.cisco.com/cpress/cc/td/cpress/fund/ith/ith01gb.htm#10053. INTERNET. Accessed March 16, 2000.

[1.3] Farely, Tom. "Digital Wireless Basics," available from http://www.privateline.com/PCS/Multiplexing.htm. INTERNET. Accessed March 16, 2000.

[2.1] Liu, Yanjing; Wang, Y. X.; Zhao, Wei; Claus, Richard O.; Lenehan, Kevin; Heflin, James R. "Ionically self-assembled second-order nonlinear optical thin film materials and devices," Proc. SPIE Vol. 3330, p. 75-79, Smart Structures and Materials 1998: Sensory Phenomena and Measurement Instrumentation for Smart Structures and Materials, Richard O. Claus; William B. Spillman; Eds. 07/1998.

[2.2] Claus, Richard O.; Holton, Carvel E.; Zhao, Wei, "Performance of optical fiber sensors embedded in polymer matrix composites for 15 years," Proc. SPIE Vol. 3330, p. 8-11, Smart Structures and Materials 1998: Sensory Phenomena and Measurement Instrumentation for Smart Structures and Materials, Richard O. Claus; William B. Spillman; Eds. 07/1998.

[2.3] Liu, Yanjing; Zhao, Wei; Wang, Y. X.; Claus, Richard O. "Functionally tailored nanoparticle-based ionically self-assembled multilayer thin films," Proc. SPIE Vol. 3324, p. 45-48, Smart Structures and Materials 1998: Smart Materials Technologies, Manfred Wuttig; Ed. 07/1998.

[2.4] Meller, Scott A.; De Vries, Marten J.; Arya, Vivek; Claus, Richard O.; Zabaronick, Noel, "Advances in optical fiber sensors for vehicle detection," Proc. SPIE Vol. 3207, p. 318-322, Intelligent Transportation Systems, Marten J. de Vries; Pushkin Kachroo; Kaan Ozbay; Alan C. Chachich; Eds. 01/1998.

[2.5] Ki Dong Oh, J. Ranade, V. Arya, A. Wang and R. O. Claus, "Fiber Optic EFPI-based Sensor for Low Magnetic Field Measurement," IEEE/LEOS Conference Proc., vol.1, pp. 236-237, 1996.

[2.6] Ki Dong Oh, J. Ranade, V. Arya, A. Wang and R. O. Claus, "Optical Fiber Fabry-Perot Interferometric Sensor for Magnetic Field Measurement," IEEE Photo. Tech. Letters, vol. 9, no. 6, pp. 797-799, June 1997.

[2.7] Oh, Ki D.; Ranade, Jaydeep; Arya, Vivek; Wang, Anbo; Claus, Richard O., "Miniaturized fiber optic magnetic field sensors," Proc. SPIE Vol. 3538, p. 136-142, Process Monitoring with Optical Fibers and Harsh Environment Sensors, Michael A. Marcus; Anbo Wang; Eds., 01/1999.

[2.8] Claus, Richard O. "Optical fiber instrumentation and applications," Proc. SPIE Vol. 3242, p. 20-24, Smart Electronics and MEMS, Ahsan Hariz; Vijay K. Varadan; Olaf Reinhold; Eds. 11/1997.

[2.9] Li, Tianchu; May, Russell G.; Wang, Anbo; Claus, Richard O. "Multimode interference and a white light scanning Michelson interferometer with a 400-mm sapphire fiber sensing head," Proc. SPIE Vol. 3555, p. 217-224, Optical and Fiber Optic Sensor Systems, Shangliang Huang; Kim D. Bennett; David A. Jackson; Eds. 08/1998.

[2.10] May, Russell G.; Shinpaugh, Kevin A.; Duncan, Paul G.; Loos, Alfred C.; Claus, Richard O. "Multifunctional fiber optic sensor for manufacturing of thermoset matrix composite materials," Proc. SPIE Vol. 3044, p. 244-251, Smart Structures and Materials 1997: Industrial and Commercial Applications of Smart Structures Technologies, Janet M. Sater; Ed. 05/1997.

[2.11] Meller, Scott A.; Zabaronick, Noel; Ghoreishian, I.; Allison, J.; Arya, Vivek; De Vries, Marten J.; Claus, Richard O. Performance of fiber optic vehicle sensors for highway axle detection: Proc. SPIE Vol. 2902, p. 166-172, "Transportation Sensors and Controls: Collision Avoidance, Traffic," Management, and ITS, Alan C. Chachich; Marten J. De Vries; Eds. 02/1997.

[2.12] May, Russell G.; Claus, Richard O. Proc. SPIE Vol. 2948, p. 24-34, Nondestructive Evaluation for Process Control in Manufacturing, Richard H. Bossi; Tom Moran; Eds. Publication Date: 11/1996.

[2.13] Arregui, Francisco J.; Lenahan, Kristie M.; Liu, Yanjing; Matias, Ignacio R.; ; Claus, Richard O. "Self-assembled optical fiber sensors," Proc. SPIE Vol. 3670, p. 74-81, Smart Structures and Materials 1999: Sensory Phenomena and Measurement Instrumentation for Smart Structures and Materials, Richard O. Claus; William B. Spillman; Eds. 05/1999.

[2.14] Kostic, Igor A.; Holton, Carvel E.; Claus, Richard O. "Optical fiber magnetic field sensors and signal processing for vehicle detection and classification," Proc. SPIE Vol. 3525, p. 381-392, Mobile Robots XIII and Intelligent Transportation Systems, Howie M. Choset; Douglas W. Gage; Pushkin Kachroo; Mikhail A. Kourjanski; Marten J. de Vries; Eds. 01/1999.

[2.15] Oh, Ki D.; Ranade, Jaydeep; Arya, Vivek; Wang, Anbo; Claus, Richard O. "Miniaturized fiber optic magnetic field sensors," Proc. SPIE Vol. 3538, p. 136-142, Process Monitoring with Optical Fibers and Harsh Environment Sensors, Michael A. Marcus; Anbo Wang; Eds. 01/1999.

[2.16] Zhao, Wei; Claus, Richard O., "Long-period grating fiber sensor with fiber Bragg grating demodulator" Proc. SPIE Vol. 3330, p. 231-236, Smart Structures and Materials 1998: Sensory Phenomena and Measurement Instrumentation for Smart Structures and Materials, Richard O. Claus; William B. Spillman; Eds. 07/1998.

[2.17] Whitesel, H.K., Sarkady, A. A., Overby, J.K., Jacobson, C.P., "Code Division Multiplexing of Fiber Optic Sensors with LED Sources," Photonics West, SPIE San Jose, February 1997.

[2.18] Bhatnagar, M,, "Multiplexing of interferometric fiber optic sensors for smart structure applications using spread spectrum system techniques," Master's Thesis, Virginia Tech, 1994.

[2.19] Mlodzianowski, D. Uttamchandani, and B. Culshaw, "Multiplexing System for Frequency Modulated Fibre Optic Sensors Using Pseudorandom Sequences," Fiber Optic Sensors III, SPIE Vol 1011, 1988, pp 26-29.

[2.20] Kersey, A. D., A. Dandridge, and M. A. Davis, "Code-Division Multiplexed Interferometric Array With Phase Noise Reduction and Low Crosstalk," 1992 Optical Fiber Sensors, IEEE and Optical Society of America, January 1992, pp 266-269.

[2.21] Street, A. M. And D. J. Edwards, "Bandwidth Requirements for M-Sequence Codes Used in Fibre Optic Multiplexing Systems," IEE Proc.-Optoelectron., Vol 142, No 4, August 1995, pp 202-206.

[2.22] Walker, J. C., R. Holms, and G. R. Jones, "Network of 12 Optical Sensors Using Code-Division Multiplexing," Electronic Letters, Vol 28, No 22, 22 October 1992, pp 2074-2075.

[2.23] Dixon, R.C., Spread Spectrum Systems, 3rd Edition, Wiley and Sons, 1994.

[3.1] "Microelectromechanical Systems Opportunities", Defense Advanced Research Projects Agency Publication, 1994.

[3.2] ADXL-50 Specification Sheet, Analog Devices, Inc., Norwood, MA, 1996.

[3.3] Koester, D.A., Rameswamy, M., Shishkoff, A., Markus, K.W., SmartMUMPs Design Handbook, MEMS Technology Application Center, (now Cronos Integrated Microsystems) MCNC, Research Triangle Park, NC, 1996.

[3.4] ADXL-05 Specification Sheet, Analog Devices, Inc., Norwood, MA, 1996.

[3.5] Dixon, R.C., Spread Spectrum Systems, 3rd Edition, Wiley and Sons, 1994.

[4.1] Porat, B., A Course in Digital Signal Processing, Wiley and Sons, 1997.

[4.2] Stremler, F. G., Introduction to Communication Systems (3rd ed), Addison-Wesley, 1996.

[7.1] Navy Small Business Innovation Research topic N97-052,"Fiber Optic Multiplexer for Distributed MEMS Sensors," 1997.

[7.2] Navy Small Business Innovation Research topic N97-055, "All Optical Shipboard Sensing System," 1997.

[7.3] Jacobson, C, P., "U.S. Navy Fiber Optic Sensor Technology," Photonics West, SPIE, San Jose, February 1997.

Vita

Carl P. Jacobson and was born in Phoenix, Arizona, and graduated from Arizona State University where he received the Bachelor of Science Degree in Engineering in 1974. He received the Master of Science Degree in Electrical Engineering from Virginia Tech in 1990.

Mr. Jacobson has worked for over twenty-five years as an engineer in high technology. His areas of expertise include stress analysis, fiber optic sensing, microelectromechanical systems (MEMS) and communications. He has authored several papers in each of these areas.

.